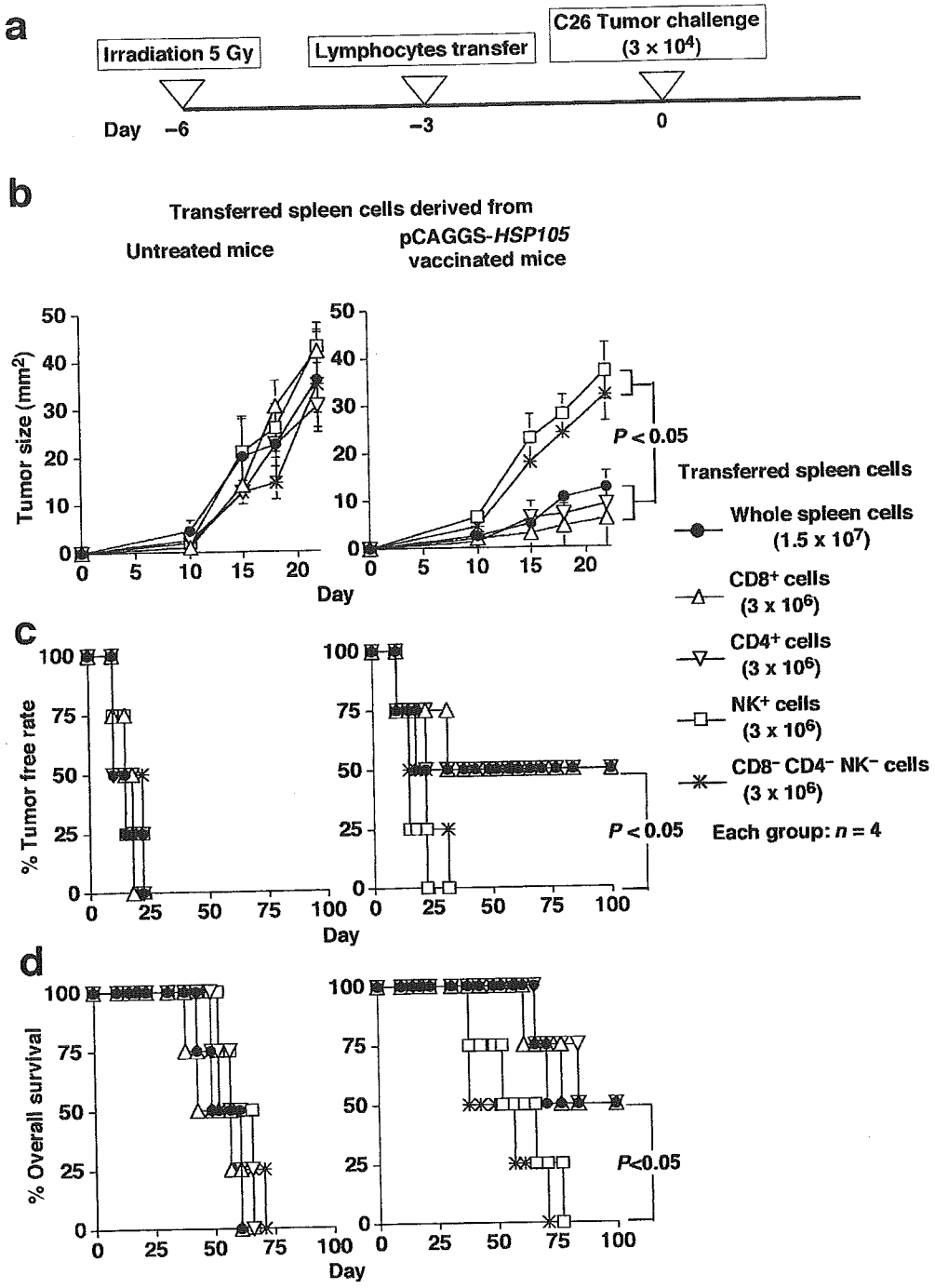

Fig. 5. Injection of either CD4⁺ T cells or CD8⁺ T cells sensitized with *HSP105* DNA vaccine into sublethally irradiated mice elicited effective antitumor adoptive immunity. (a) Experimental protocol; each group consisted of four mice. (b) Suppression of the growth of HSP105-expressing C26 tumors inoculated subcutaneously into mice transferred with each group of spleen cells. Tumor area was calculated as the product of width and length. The result is presented as the mean area of tumor ± SE, and we evaluated the statistical significance using the unpaired *t*-test. (c,d) Percentage tumor free rate (c) and percentage overall survival (d) were calculated using the Kaplan–Meier method, and the statistical significance of differences in survival time between groups was evaluated using Wilcoxon's test.

mice did not cause the mice to reject challenges with C26 cells (3×10^4). Conversely, two of the four mice (50%) that were treated with whole spleen cells, CD8⁺ T cells, or CD4⁺ T cells derived from *HSP105* DNA-vaccinated mice completely rejected challenges with C26 cells (3×10^4; Fig. 5b–d). Thus, sublethally irradiated lymphopenic mice transfused with CD4⁺ T cells or CD8⁺ T cells derived from *HSP105* DNA-vaccinated mice displayed tumor growth inhibition. These results suggest that both CD4⁺ and CD8⁺ T cells play critical roles in antitumor immunity induced by immunization with

 doi: 10.1111/j.1349-7006.2005.00093.x

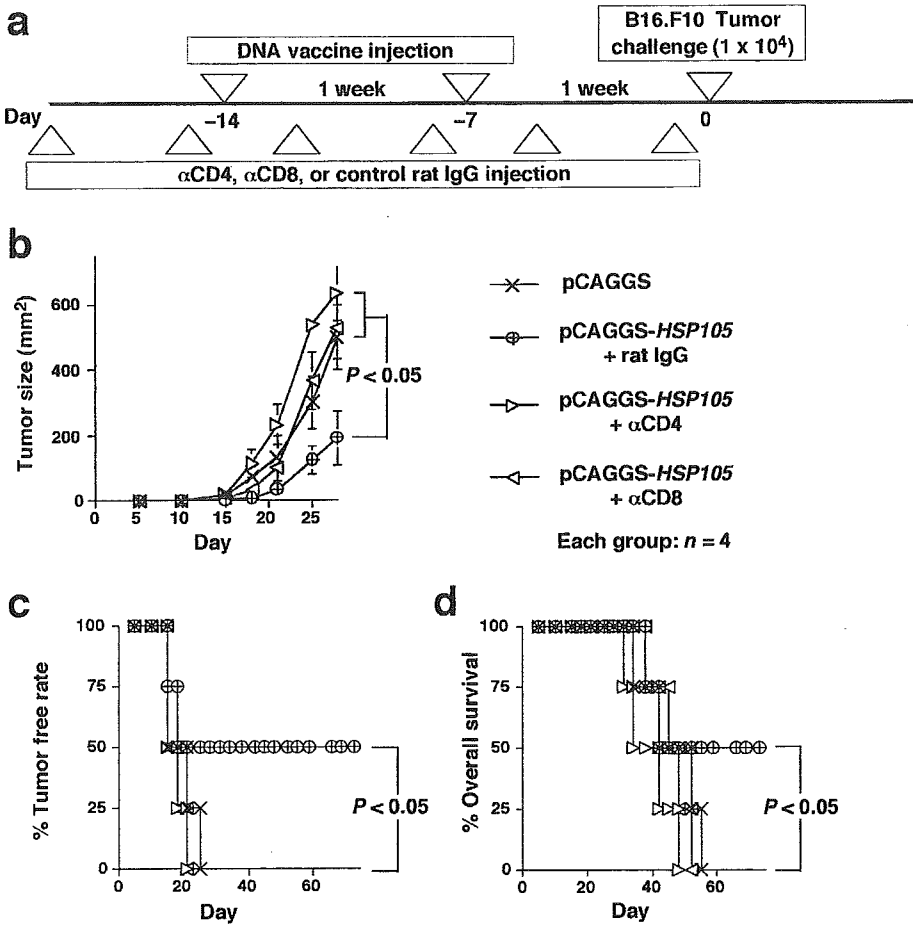

Fig. 6. Involvement of both CD4⁺ T cells and CD8⁺ T cells in protection against B16.F10 induced by vaccination with *HSP105* DNA. (a) Experimental protocol for *in vivo* depletion of CD4⁺ T cells and CD8⁺ T cells. Each group consisted of four mice. (b) Suppression of the growth of HSP105-expressing B16.F10 tumors inoculated subcutaneously into mice vaccinated with *HSP105* DNA. Tumor area was calculated as the product of width and length. Data are presented as mean area of tumor ± SE, and we evaluated the statistical significance using the unpaired *t*-test. (c,d) Percentage tumor free rate (c) and percentage overall survival (d) were calculated using the Kaplan–Meier method, and the statistical significance of differences in survival time between groups was evaluated using Wilcoxon's test.

the *HSP105* DNA-vaccine. The mice shown in Figure 5 were killed more than 100 days after lymphocyte transfer, respectively. All mice were apparently healthy and without abnormalities, suggesting autoimmunity for, for example, dermatitis, arthritis, or neurological disorders. The brain, liver, lung, heart, kidney, and spleen tissues of *HSP105* DNA-immunized mice were critically scrutinized and compared with those of normal mice. These tissues had normal structures and cellularity for each of the two groups examined, and pathological changes caused by immune response, such as CD8⁺ or CD4⁺ T lymphocyte infiltration or tissue destruction and repair, were not present, as shown in Figure 4b. These results indicate that T cells stimulated with HSP105 do not recognize normal cells that express HSP105 at physiological levels.

Involvement of both CD4⁺ T cells and CD8⁺ T cells in protection against B16.F10 induced by *HSP105* DNA-vaccination

To determine the role of CD4⁺ T cells and CD8⁺ T cells in the protection against B16.F10 tumor cells induced by *HSP105* DNA-vaccination, we depleted mice of CD4⁺ T cells or CD8⁺ T cells by treatment with anti-CD4 or anti-CD8 mAb *in vivo*. More than 90% of CD4⁺ T cells or CD8⁺ T cells were depleted (data not shown). During this procedure, mice were immunized with DNA vaccine and challenged with B16.F10 cells (Fig. 6a). Depletion of either CD4⁺ T cells or CD8⁺ T cells almost totally abrogated the protective immunity induced by immunization with *HSP105* DNA vaccine (Fig. 6b–d). These results suggest that both CD4⁺ T cells and CD8⁺ T cells play critical roles in antitumor immunity induced by immunization with *HSP105* DNA vaccine.

Discussion

Advances in molecular biology and tumor immunology have paved the way for identification of a large number of genes encoding TAA and antigenic peptides recognized by tumor-reactive CTL, hence peptide-based cancer immunotherapy has been the focus of much research.[24–26] However, current clinical trials for peptide-based immunotherapy have rarely resulted in tumor regression.[27] The immunogenicity of these

tumor antigenic peptides or the vaccination strategy may be sufficient to induce CTL responses but not to elicit $CD4^+$ T cells.

DNA-based immunization is potentially a powerful method for immunizing against microbial, viral, and tumor antigens through both humoral and cell-mediated immune responses.[28] The generation of T-cell immunity involves local target cell transfection and protein antigen production, which is taken up by host APC, leading to cross-presentation in draining lymph nodes; in addition, direct DNA transfection into APC in peripheral tissue has also been demonstrated.[29] Compared with orthodox vaccines consisting of tumor proteins or viral components, DNA vaccination stimulates host immunity against transgene-encoding proteins without the processes related to protein purification. In the present study, a DNA vaccine was used to activate HSP105-specific tumor immunity.

Although the SEREX method facilitated the identification of tumor antigens that could be recognized by antibodies and $CD4^+$ Th cells, few of their T cell epitopes have been determined.[2,30] We previously reported that HSP105, identified by SEREX of pancreatic adenocarcinoma, was overexpressed specifically in a variety of human cancers, including pancreatic and colon adenocarcinoma.[1,5] Other investigators identified HSP105 by SEREX using other cDNA libraries derived from tissues including colorectal cancer, melanoma, and normal testis. HSP105 are complexes associated with HSP70/HSC70,[31,32] which negatively regulate HSP70/HSC70 chaperone activity.[33] In addition, HSP105 protects neuronal cells against the apoptosis induced by various stresses.[34] HSP105 consists of HSP105α and HSP105β. HSP105α is a constitutively expressed 105-kDa HSP that is induced by a variety of stresses, whereas HSP105β is a 90-kDa HSP that is specifically induced by heat shock at 42°C. HSP105β is a truncated form of HSP105α.[12] We used in this study the mouse HSP105α DNA and protein. Recently, Subjeck and colleagues reported that recombinant HSP110 and cancer antigens such as Her2/*neu* or gp100 complexes are powerful cancer vaccines.[8,9,35] Their HSP110[11] and our HSP105α are in fact the same protein.

Although they noted that HSP110 did not have immunogenic properties, we emphasize in this study that HSP105 does have a strong immunogenic action. Although we did not identify the HSP105-derived epitope peptides of $CD8^+$ T-cells or $CD4^+$ T-cells in this study, we did prove that HSP105 itself could induce both $CD4^+$ T-cells and $CD8^+$ T-cells to become reactive to tumor cells expressing HSP105. As shown in Figure 5, in a homeostatic lymphocyte proliferation model, we demonstrated that adoptive transfer of either $CD4^+$ T cells or $CD8^+$ T cells alone into sublethally irradiated mice was sufficient to reject C26 cells that do not express MHC class II molecules. To ascertain whether this is also true for B16.F10 that express both MHC class I and II molecules in the presence of interferon (IFN)-γ, further investigation is needed. As shown in Figure 6, we demonstrated that both $CD4^+$ T cells and $CD8^+$ T cells were required for rejection of B16.F10 in the induction phase. In terms of the mechanism for the rejection of C26 tumors, we have other data relating to vaccination with HSP105 protein-pulsed BM-DC instead of *HSP105* DNA vaccination. In those experiments, we also demonstrated that both $CD4^+$ T cells and $CD8^+$ T cells were required for rejection of not only B16.F10 but also C26 in the induction phase by depleting $CD4^+$ T cells and $CD8^+$ T cells using the *in vivo* administration of antibodies (unpublished data). Therefore, both HSP105-specific $CD4^+$ T cells and $CD8^+$ T cells seem to be important for the rejection of HSP105-expressing tumors in the induction phase, and either $CD4^+$ T cells or $CD8^+$ T cells can independently exert anti-C26 tumor effects in the effector phase in a homeostatic lymphocyte proliferation model.

It has been reported that antigen-specific $CD4^+$ T-cell help is required to activate memory $CD8^+$ T cells to fully functional effector killer cells.[36] The peptides derived from exogenous antigens acquired by endocytosis are typically presented on MHC class II molecules on the surface of APC, and activate $CD4^+$ T cells. We observed in this study that $CD4^+$ T cells specific to HSP105, in fact, have an important role in tumor rejection, even when tumors do not express MHC class II molecules, such as the C26 tumors used in this study. It was recently reported that tumor-specific $CD4^+$ T cells may have a pivotal role in preventing early tumorigenesis by secreting IFN-γ and stimulating the classical macrophage-activation pathway. This results in the inhibition of tumor cell growth, even when tumor cells themselves do not express MHC class II molecules.[37] To better understand the mechanism of C26 tumor rejection by HSP105-specific $CD4^+$ T cells, further studies are needed. Furthermore, peptides derived from exogenous self-antigen, HSP105, acquired by endocytosis are possibly presented by MHC class I molecules on the surface of APC by cross-presentation to activate $CD8^+$ T cells.

Because HSP are present in all organisms, low levels of human HSP-derived peptides serve as harbingers of autoimmune responses after CTL have been primed to respond to bacterial HSP-derived peptides.[38] However, because many cancers overexpress HSP, CTL-based vaccines that elicit an anti-HSP response might be effective against many different tumors.[39] Indeed, in this study, HSP105 itself evoked T-cell-mediated tumor rejection without autoimmune reactions. In the present paper, all results shown in the figures were obtained using female mice, but we have carried out the same experiment using male mice. *HSP105* DNA vaccination did not induce T-cell infiltration or damage in testis tissue (in which HSP105 is highly expressed). Furthermore, *HSP105* DNA vaccination was also able to induce antitumor immunity in male mice (data not shown), indicating that male mice did not acquire immunological tolerance to HSP105 expressed in testis tissue.

To substantiate the specificity for HSP105, we searched for mouse cancer cell lines derived from BALB/c mice and C57BL/6 mice that do not express HSP105. However, all cancer cell lines we examined strongly expressed HSP105. BALB/3T3 fibroblasts expressed HSP105 relatively weakly, but these cells unfortunately did not form tumors in mice. Further investigations are needed to clarify whether *HSP105* DNA vaccination affects the growth of some tumors that do not express HSP105.

We showed in this study that *HSP105* DNA vaccination can prime T cells to be reactive to tumor cells expressing HSP105 *in vivo*, and that growth of C26 and B16.F10 cells expressing HSP105 was prevented without inducing autoimmune destruction in murine subcutaneous CRC and melanoma models. We believe that *HSP105* DNA vaccination is a novel strategy for the prevention of CRC and melanoma in patients treated surgically who are at high risk of recurrence

 doi: 10.1111/j.1349-7006.2005.00093.x

of CRC or melanoma. Whether or not HSP105 is an ideal target for immunotherapy in human cancers will continue to be investigated in our laboratory.

Acknowledgments

We thank Drs Hidetake Matsuyoshi, Shinya Hirata, Yoshiaki Ikuta, and Daiki Fukuma (Department of Immunogenetics, Graduate School of Medical Sciences, Kumamoto University) for technical assistance, Dr Junichi Miyazaki, Osaka University, for providing the pCAGGS vector, and Dr Kyoichi Shimomura (Fujisawa Pharmaceutical Co.), for providing the cell line. This work was supported in part by Grants-in-Aid (no. 12213111 to Y. Nishmura, and no. 14770142 to T. Nakatsura) from the Ministry of Education, Science, Technology, Sports and Culture, Japan.

References

1 Nakatsura T, Senju S, Yamada K, Jotsuka T, Ogawa M, Nishimura Y. Gene cloning of immunogenic antigens overexpressed in pancreatic cancer. *Biochem Biophys Res Commun* 2001; **281**: 936–44.
2 Nakatsura T, Senju S, Ito M, Nishimura Y, Itoh K. Cellular and humoral immune responses to a human pancreatic cancer antigen, coactosin-like protein, originally defined by the SEREX method. *Eur J Immunol* 2002; **32**: 826–36.
3 Monji M, Senju S, Nakatsura T *et al.* Head and neck cancer antigens recognized by the humoral immune system. *Biochem Biophys Res Commun* 2002; **294**: 734–41.
4 Monji M, Nakatsura T, Senju S *et al.* Identification of a novel human cancer/testis antigen, KM-HN-1, recognized by cellular and humoral immune responses. *Clin Cancer Res* 2004; **10**: 6047–57.
5 Kai M, Nakatsura T, Egami H, Senju S, Nishimura Y, Ogawa M. Heat shock protein 105 is overexpressed in a variety of human tumors. *Oncol Rep* 2003; **10**: 1777–82.
6 Srivastava P. Interaction of heat shock proteins with peptides and antigen presenting cells: chaperoning of the innate and adaptive immune responses. *Annu Rev Immunol* 2002; **20**: 395–425.
7 Hickman-Miller HD, Hildebrand WH. The immune response under stress. The role of HSP-derived peptides. *Trends Immunol* 2004; **25**: 427–33.
8 Manjili MH, Henderson R, Wang XY *et al.* Development of a recombinant HSP110-HER-2/neu vaccine using the chaperoning properties of HSP110. *Cancer Res* 2002; **62**: 1737–42.
9 Wang XY, Chen X, Manjili MH, Repasky E, Henderson R, Subjeck JR. Targeted immunotherapy using reconstituted chaperone complexes of heat shock protein 110 and melanoma-associated antigen gp100. *Cancer Res* 2003; **63**: 2553–60.
10 Wang XY, Li Y, Manjili MH, Repasky EA, Pardoll DM, Subjeck JR. Hsp110 over-expression increases the immunogenicity of the murine CT26 colon tumor. *Cancer Immunol Immunother* 2002; **51**: 311–9.
11 Lee-Yoon D, Easton D, Murawski M, Burd R, Subjeck JR. Identification of a major subfamily of large hsp70-like proteins through the cloning of the mammalian 110-kDa heat shock protein. *J Biol Chem* 1995; **270**: 15725–33.
12 Yasuda K, Nakai A, Hatayama T, Nagata K. Cloning and expression of murine high molecular mass heat shock proteins, HSP105. *J Biol Chem* 1995; **270**: 29718–23.
13 Ishihara K, Yasuda K, Hatayama T. Molecular cloning, expression and localization of human 105 kDa heat shock protein, hsp105. *Biochim Biophys Acta* 1999; **1444**: 138–42.
14 Hattori K, Matsushita R, Kimura K, Abe Y, Nakashima E. Synergistic effect of indomethacin with adriamycin and cisplatin on tumor growth. *Biol Pharm Bull* 2001; **24**: 1214–7.
15 Nakatsura T, Kageshita T, Ito S *et al.* Identification of glypican-3 as a novel tumor marker for melanoma. *Clin Cancer Res* 2004; **10**: 6612–21.
16 Yoshitake Y, Nakatsura T, Monji M *et al.* Proliferation potential-related protein, an ideal esophageal cancer antigen for immunotherapy, identified using complementary DNA microarray analysis. *Clin Cancer Res* 2004; **10**: 6437–48.
17 Nakatsura T, Komori H, Kubo T *et al.* Mouse homologue of a novel human oncofetal antigen, glypican-3, evokes T cell-mediated tumor rejection without autoimmune reactions in mice. *Clin Cancer Res* 2004; **10**: 8630–40.
18 Matsuyoshi H, Senju S, Hirata S, Yoshitake Y, Uemura Y, Nishimura Y. Enhanced priming of antigen-specific CTLs in vivo by embryonic stem cell-derived dendritic cells expressing chemokine along with antigenic protein: application to antitumor vaccination. *J Immunol* 2004; **172**: 776–86.
19 Maruyama H, Higuchi N, Nishikawa Y *et al.* High-level expression of naked DNA delivered to rat liver via tail vein injection. *J Gene Med* 2002; **4**: 333–41.
20 Hylander BL, Chen X, Graf PC, Subjeck JR. The distribution and localization of hsp110 in brain. *Brain Res* 2000; **869**: 49–55.
21 Dummer W, Niethammer AG, Baccala R *et al.* T cell homeostatic proliferation elicits effective antitumor autoimmunity. *J Clin Invest* 2002; **110**: 185–92.
22 Maine GN, Mule JJ. Making room for T cells. *J Clin Invest* 2002; **110**: 157–9.
23 Dudley ME, Wunderlich JR, Robbins PF *et al.* Cancer regression and autoimmunity in patients after clonal repopulation with antitumor lymphocytes. *Science* 2002; **298**: 850–4.
24 van der Bruggen P, Traversari C, Chomez P *et al.* A gene encoding an antigen recognized by cytolytic T lymphocytes on a human melanoma. *Science* 1991; **254**: 1643–7.
25 Kawakami Y, Eliyahu S, Delgado CH *et al.* Identification of a human melanoma antigen recognized by tumor-infiltrating lymphocytes associated with in vivo tumor rejection. *Proc Natl Acad Sci USA* 1994; **91**: 6458–62.
26 Chen YT, Gure AO, Tsang S *et al.* Identification of multiple cancer/testis antigens by allogeneic antibody screening of a melanoma cell line library. *Proc Natl Acad Sci USA* 1998; **95**: 6919–23.
27 Rosenberg SA, Yang JC, Schwartzentruber DJ *et al.* Immunologic and therapeutic evaluation of a synthetic peptide vaccine for the treatment of patients with metastatic melanoma. *Nat Med* 1998; **4**: 321–7.
28 Kumar V, Sercarz E. Genetic vaccination: the advantages of going naked. *Nat Med* 1996; **2**: 857–9.
29 Leitner WW, Ying H, Restifo NP. DNA and RNA-based vaccines: principles, progress and prospects. *Vaccine* 1999; **18**: 765–77.
30 Jager E, Chen YT, Drijfhout JW *et al.* Simultaneous humoral and cellular immune response against cancer-testis antigen NY-ESO-1: definition of human histocompatibility leukocyte antigen (HLA)-A2-binding peptide epitopes. *J Exp Med* 1998; **187**: 265–70.
31 Wakatsuki T, Hatayama T. Characteristic expression of 105-kDa heat shock protein (HSP105) in various tissues of nonstressed and heat-stressed rats. *Biol Pharm Bull* 1998; **21**: 905–10.
32 Hatayama T, Yasuda K. Association of HSP105 with HSC70 in high molecular mass complexes in mouse FM3A cells. *Biochem Biophys Res Commun* 1998; **248**: 395–401.
33 Yamagishi N, Nishihori H, Ishihara K, Ohtsuka K, Hatayama T. Modulation of the chaperone activities of Hsc70/Hsp40 by Hsp105alpha and Hsp105beta. *Biochem Biophys Res Commun* 2000; **272**: 850–5.
34 Hatayama T, Yamagishi N, Minobe E, Sakai K. Role of hsp105 in protection against stress-induced apoptosis in neuronal PC12 cells. *Biochem Biophys Res Commun* 2001; **288**: 528–34.
35 Manjili MH, Wang XY, Chen X *et al.* HSP110-HER2/neu chaperone complex vaccine induces protective immunity against spontaneous mammary tumors in HER-2/neu transgenic mice. *J Immunol* 2003; **171**: 4054–61.
36 Gao FG, Khammanivong V, Liu WJ, Leggatt GR, Frazer IH, Fernando GJ. Antigen-specific $CD4^+$ T-cell help is required to activate a memory $CD8^+$ T cell to a fully functional tumor killer cell. *Cancer Res* 2002; **62**: 6438–41.
37 Corthay A, Skovseth DK, Lundin KU *et al.* Primary antitumor immune response mediated by $CD4^+$ T cells. *Immunity* 2005; **22**: 371–83.
38 Zugel U, Schoel B, Yamamoto S, Hengel H, Morein B, Kaufmann SH. Cross recognition by CD8 T cell receptor alpha beta cytotoxic T lymphocytes of peptides in the self and the mycobacterial hsp60 which share intermediate sequence homology. *Eur J Immunol* 1995; **25**: 451–8.
39 Faure O, Graff-Dubois S, Bretaudeau L *et al.* Inducible Hsp70 as target of anticancer immunotherapy: Identification of HLA-A*0201-restricted epitopes. *Int J Cancer* 2004; **108**: 863–70.

ELSEVIER

Journal of the Neurological Sciences 243 (2006) 21 – 30

Journal of the Neurological Sciences

www.elsevier.com/locate/jns

Upregulation of vascular growth factors in multiple sclerosis: Correlation with MRI findings

Jen Jen Su [a], Manabu Osoegawa [a], Takeshi Matsuoka [a], Motozumi Minohara [a], Masahito Tanaka [a], Takaaki Ishizu [a], Futoshi Mihara [b], Takayuki Taniwaki [a], Jun-ichi Kira [a,*]

[a] *Department of Neurology, Neurological Institute, Graduate School of Medical Sciences, Kyushu University, Fukuoka, 812-8582, Japan*
[b] *Department of Radiology, Graduate School of Medical Sciences, Kyushu University, Fukuoka, Japan*

Received 10 June 2005; received in revised form 13 October 2005; accepted 9 November 2005
Available online 27 December 2005

Abstract

Vascular permeability changes precede the development of demyelinating lesions in multiple sclerosis (MS), and vessel wall thickening and capillary proliferation are frequently seen in autopsied MS lesions. Although vascular growth factors are critical for inducing such vascular changes, their involvement in MS has not been extensively studied. Thus, we examined the involvement of various vascular growth factors in MS according to their clinical phase and subtype. We measured serum levels of vascular endothelial growth factor (VEGF), acidic and basic fibroblast growth factors (FGF) and platelet-derived growth factors (PDGFs)-AA, -AB and -BB in 50 patients with MS (27 opticospinal MS and 23 conventional MS patients) and 33 healthy controls using sandwich enzyme immunoassays. Correlations between growth factor changes and brain and spinal cord MRI findings were then analyzed. Serum VEGF concentrations were significantly higher in MS patients in relapse than in controls ($p=0.0495$) and in MS patients in remission ($p=0.0003$), irrespective of clinical subtype. Basic FGF was significantly increased in conventional MS patients, but not opticospinal MS patients compared with controls ($p=0.0291$), irrespective of clinical phase. VEGF at relapse showed a significant positive correlation with the length of spinal cord lesions on MRI ($r=0.506$, $p=0.0319$). The results suggest that an increase in serum VEGF concentration might be involved in MS relapse and the formation of longitudinally extensive spinal cord lesions.

Keywords: OS-MS; C-MS; VEGF; FGF; MRI; Longitudinally extensive spinal cord lesion

1. Introduction

Multiple sclerosis (MS) is an inflammatory demyelinating disease of the central nervous system (CNS). Although the pathological hallmark of this disease is primarily demyelination, a wide variety of pathological changes, such as axonal degeneration, gliosis, remyelination and vascularization, have been noted. In particular, vascular permeability changes are considered crucial since they precede the development of MS lesions [1] and lesions preferentially develop perivascularly [2,3]. However, the precise mechanisms and the molecules responsible for the vascular changes observed in MS are not fully understood [3].

Growth factors are critical for inducing tissue growth and remodeling. Vascular endothelial growth factor (VEGF) induces vascular proliferation as well as vascular permeability changes [4], while platelet-derived growth factor (PDGF) and fibroblast growth factor (FGF) not only induce oligodendroglial progenitor cell growth [5] but also contribute to angiogenesis [6]. Although recent pathological studies have revealed upregulation of VEGF in MS plaques [7], the involvement of growth factors that potentially induce angiogenesis has not been extensively studied in accord with clinical phase and MRI findings.

Two subtypes of MS, distinct in the nature of their CNS pathology, exist in Asians, namely, opticospinal MS (OS-MS) and conventional MS (C-MS). Selective involvement of the optic nerves and spinal cord, and tissue necrosis and conspicuous vascular components are seen in OS-MS, while

* Corresponding author. Tel.: +81 92 642 5340; fax: +81 92 642 5352.
E-mail address: kira@neuro.med.kyushu-u.ac.jp (J. Kira).

0022-510X/$ - see front matter © 2005 Elsevier B.V. All rights reseved.
doi:10.1016/j.jns.2005.11.006

disseminated involvement of the CNS and perivascular demyelination are seen in C-MS [8–10]. These observations prompted us to study serum levels of various growth factors, which might contribute to the vascular changes observed in MS, according to clinical phase and subtype. In addition, we analyzed the correlation between growth factor changes and brain and spinal cord MRI findings, which are distinct between the two subtypes.

2. Subjects and methods

2.1. Subjects

A total of 50 consecutive patients (9 men and 41 women) with relapsing remitting MS, diagnosed according to the criteria of McDonald et al. [11] at the Department of Neurology, Kyushu University Hospital between September 1996 and May 2004, were enrolled in the present study after informed consent was obtained. None were receiving immunomodulatory therapies (interferon beta or immunosuppressants) or high dose corticosteroids (more than 15 mg prednisolone per day) at the time of blood sampling. The mean age at examination was 41.6±16.0 years (mean±S.D.) (range: 17 to 89) and the mean age at disease onset was 33.1±16.2 years (range: 10 to 89). The age at onset and examination had a significant positive correlation ($r=0.751$, $p<0.0001$). All patients were clinically classified as OS-MS or C-MS before sandwich enzyme immunoassays were performed. Briefly, 27 patients whose clinically estimated main lesions were confined to the optic nerves and spinal cord were classified as OS-MS [12]. These patients had no clinical evidence of disease in either the cerebrum or cerebellum, but minor brainstem signs, such as transient double vision and nystagmus, were acceptable.

The remaining 23 patients had multiple involvements of the CNS, including the cerebrum, cerebellum and brainstem, and were classified as C-MS. Disability was evaluated throughout the study by one of the authors (M. Osoegawa) using Kurtzke's Expanded Disability Status Scale (EDSS) score [13], and the progression index (PI) was used for evaluating disease progression; this was calculated by dividing the EDSS score at the last examination by the disease duration [14]. The demographic features of the patients are summarized in Table 1. Sera were obtained at relapse (within 1 month after onset of acute relapse) or remission. Because of limitations of stocked serum volume, from among the 50 MS patients VEGF was measured in 43 samples while other vascular growth factors were also measured in 43. For VEGF assay, 24 serum samples from

Table 1
Clinical and MRI findings of MS patients in this study

	MS ($n=50$)	OS-MS ($n=27$)	C-MS ($n=23$)
Females:males**	41:9	27:0	14:9
Age at disease onset[a,*]	33.1±16.2	37.9±18.1	27.6±11.7
Age at examination[a,*]	41.6±16.0	45.8±16.5	36.7±14.0
Disease duration[a]	8.5±9.3	7.8±8.3	9.1±10.5
EDSS score before peak[b] (stable, relapse)	2.7±2.4	2.8±2.6	2.5±2.2
EDSS score at peak[b] (relapse)	4.6±1.6	4.8±1.7	4.3±1.4
EDSS score at remission[b] (relapse)	3.3±2.2	3.3±2.3	3.3±2.3
Progression index	0.7±1.5	0.8±1.9	0.6±0.8
Brain MRI:			
9 or more T2-high lesions**	28/50 (56.0%)	9/27 (33.3%)	19/23 (82.6%)
Number of T2-high lesions**	9.4±8.6	5.6±5.3	13.7±9.4
1 or more Gd-enhanced lesions	13/50 (26.0%)	5/27 (18.5%)	8/23 (34.8%)
Number of Gd-enhanced lesions	0.3±0.7	0.2±0.4	0.5±0.9
Infratentorial lesion	21/50 (42.0%)	10/27 (37.0%)	11/23 (47.8%)
Juxtacortical lesion	27/50 (54.0%)	12/27 (44.4%)	15/23 (65.2%)
At least 3 periventricular lesions**	25/50 (50.0%)	8/27 (29.6%)	17/23 (73.9%)
Proportion of patients who fulfilled McDonald's MRI criteria*	25/50 (50.0%)	9/27 (33.3%)	16/23 (69.6%)
Number of black holes**	2.0±3.0	0.8±1.0	3.4±3.8
Spinal cord MRI:			
Frequency of spinal cord lesions	32/48 (66.7%)	19/27 (70.4%)	13/21 (61.9%)
Frequency of Gd-enhanced lesions	6/48 (12.5%)	4/27 (14.8%)	2/21 (9.5%)
Spinal cord lesion length[#]	5.0±4.9 cm	6.1±5.7 cm	3.5±3.2 cm
Longitudinally extensive spinal cord lesions	14/48 (29.2%)	11/27 (40.7%)	3/21 (14.3%)

[a]Mean±S.D. (years).
[b]Mean±S.D.
MS=multiple sclerosis; OS-MS=opticospinal MS; C-MS=conventional MS.
EDSS=Expanded Disability Status Scale of Kurtzke; Gd=gadolinium.
*$p<0.05$, **$p<0.01$, for the comparison between OS-MS and C-MS.
[#]Mean±S.D. of the spinal cord lesion length was calculated using only patients with spinal cord lesions on MRI.

23 OS-MS patients, 14 sera at relapse and 10 at remission (1 patient was examined both at relapse and remission), and 19 samples from 19 C-MS patients, 9 at relapse and 10 at remission were tested. For other vascular growth factor assays, 23 serum samples from 23 OS-MS patients, 12 at relapse and 11 at remission and 20 samples from 20 C-MS patients, 9 at relapse and 11 at remission, were examined. A total of 7 MS patients (4 OS-MS and 3 C-MS) were on low dose oral prednisolone at the time of blood sampling (Table 2). Thirty-three healthy subjects (14 men and 19 women) were enrolled as controls. Their average age at sampling was 45.1±17.8 years (range: 21 to 84 years). Age at examination was not different significantly among MS patients in relapse, those in remission and controls, and among OS-MS patients, C-MS patients and controls.

2.2. Sandwich enzyme immunoassays

VEGF, acidic and basic FGFs and PDGFs-AA, -AB and -BB were measured with quantitative sandwich enzyme immunoassays according to the manufacturer's standard protocol (R&D Systems, Minneapolis, MS, USA) by one of the authors (J. J. Su) who was unaware of the diagnoses. Serum samples were thawed from −80 °C to room temperature and assayed in duplicate for the presence of each protein in 96-well polystyrene microtiter plates coated with each capture antibody or a recombinant human PDGF-Rβ/Fc chimera. The assays used each detection antibody conjugated to horseradish peroxidase, and color was developed with tetramethylbenzidine/hydrogen peroxide. The lower detection limits for each protein were as follows: 9 pg/ml for VEGF, 5.68 pg/ml for acidic FGF, 3 pg/ml for basic FGF, 2.07 pg/ml for PDGF-AA, 1.7 pg/ml for PDGF-AB and 15 pg/ml for PDGF-BB.

2.3. Magnetic resonance imaging

All MR studies were performed using 1.5 T units, Magnetom Vision and Symphony (Siemens Medical Systems, Erlangen, Germany) within one month from blood sampling [12]. Typical imaging parameters for brain MRI were: axial T2-weighted turbo spin-echo imaging using TR/TE=2800/90 ms, flip angle=180°; axial turbo-FLAIR imaging using TI/TR/TE=2200/9000/110 ms, flip angle=180°; and sagittal and axial precontrast and axial and coronal postcontrast T1-weighted spin-echo imaging using TR/TE range=400–460/12–17 ms, flip angle range=80–90°. One excitation, a matrix of 256 × 256, a slice thickness of 5 mm, and a slice gap of 2.5 mm were used for all brain studies. Gadopentetate dimeglumine at 0.1 mmol/kg body weight was administered intravenously for contrast-enhanced studies. The typical imaging parameters of the spinal cord were as follows: sagittal T2-weighted turbo spin-echo imaging using TR/TE range=2500–2800/90–116 ms, flip angle=180°, number of excitations=3–4; sagittal T1-weighted spin-echo imaging using TR/TE range=400–440/11–12 ms, flip angle range=90–170°, number of excitations=2–3; axial T2-weighted turbo spin-echo imaging using TR/TE range=3200–5360/99–116 ms, flip angle=180°, number of excitations=3–4; axial T1-weighted spin-echo imaging using TR/TE range=400–440/12 ms, flip angle range=90–170°, number of excitations=2. For sagittal imaging, a matrix of 256 × 256 or 512 × 512, a slice thickness of 4 mm and a slice gap of 0.4 mm were used, and for axial imaging, a matrix of 256 × 256 or 512 × 512, a slice thickness of 5 mm, and a slice gap range of 1.5–5 mm were used. Brain and spinal cord MRI were evaluated independently by two of the authors (F. Mihara and M. Tanaka) who were unaware of the diagnoses. Spinal cord lesions longer than three vertebral lengths were considered longitudinally extensive. Brain MRI lesions were evaluated according to McDonald's MRI criteria for MS [11]. The interval between blood sampling and MRI scanning was less than one month in all cases examined.

2.4. Statistical analysis

The Mann–Whitney U test was used for statistical analyses of age at onset, age at blood sampling, disease

Table 2
Clinical data on steroid use of MS patient at the time of blood sampling in this study

	VEGF assay		Other vascular growth factor assay	
At relapse				
No corticosteroid	14 OS-MS		11 OS-MS	
	9 C-MS		9 C-MS	
Low dose corticoid			1 OS-MS	(1:5 mg/day)
At remission				
No corticosteroid	8 OS-MS		8 OS-MS	
	7 C-MS		10 C-MS	
Low dose corticoid	2 OS-MS	(1:5 mg every other day)	3 OS-MS	(1:10 mg/day)
		(1:15 mg/day)		(1:7.5 mg/day)
				(1:5 mg every other day)
	3 C-MS	(1:15/5 mg alternatively)	1 C-MS	(1:5 mg/day)
		(1:5 mg every other day)		
		(1:5 mg/day)		

Number of patients is shown.

duration, EDSS score, PI and length of spinal cord lesions on MRI. Statistical analyses of growth factor levels were initially performed using the Kruskal–Wallis H test for MS patients in relapse, those in remission, and controls, and for OS-MS patients, C-MS patients, and controls. When statistical significance was found, the Mann–Whitney U test was used to determine the statistical differences between each subgroup; uncorrelated p values were corrected by multiplying by the number of comparisons (Bonferroni–Dunn's correction). Spearman's rank correlation test was used to determine correlations between each vascular growth factor, and between clinical parameters and each vascular growth factor. The Chi-square test with Yates' correction or Fisher's exact probability test when the criteria were fulfilled, were used for statistical analyses of the frequency of brain and spinal cord MRI lesions. In all assays, $p<0.05$ was considered statistically significant.

3. Results

3.1. Clinical and neuroimaging findings

The proportion of females with OS-MS was significantly higher than those with C-MS ($p=0.0003$) (Table 1). Ages at disease onset and examination were also significantly higher in OS-MS than C-MS ($p=0.0149$ and $p=0.0438$, respectively). EDSS score at peak and PI were higher in OS-MS than C-MS, although the disease duration was shorter in the former than the latter, but none of these differences reached

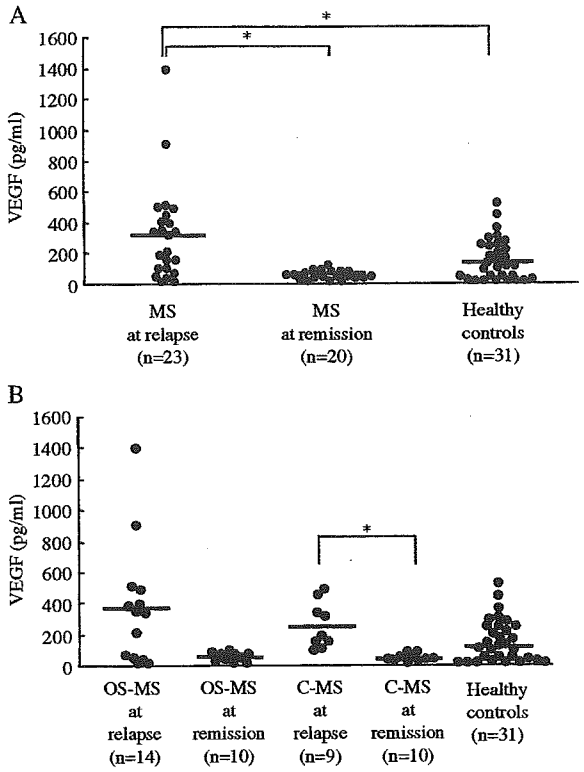

Fig. 2. (A) VEGF concentration in sera of MS patients analyzed separately according to their clinical phase. Bars indicate the mean of each group. *$p<0.05$. (B) VEGF concentration in sera from MS patients analyzed separately according to their clinical subtype and clinical phase. Bars indicate the mean of each group. *$p<0.05$.

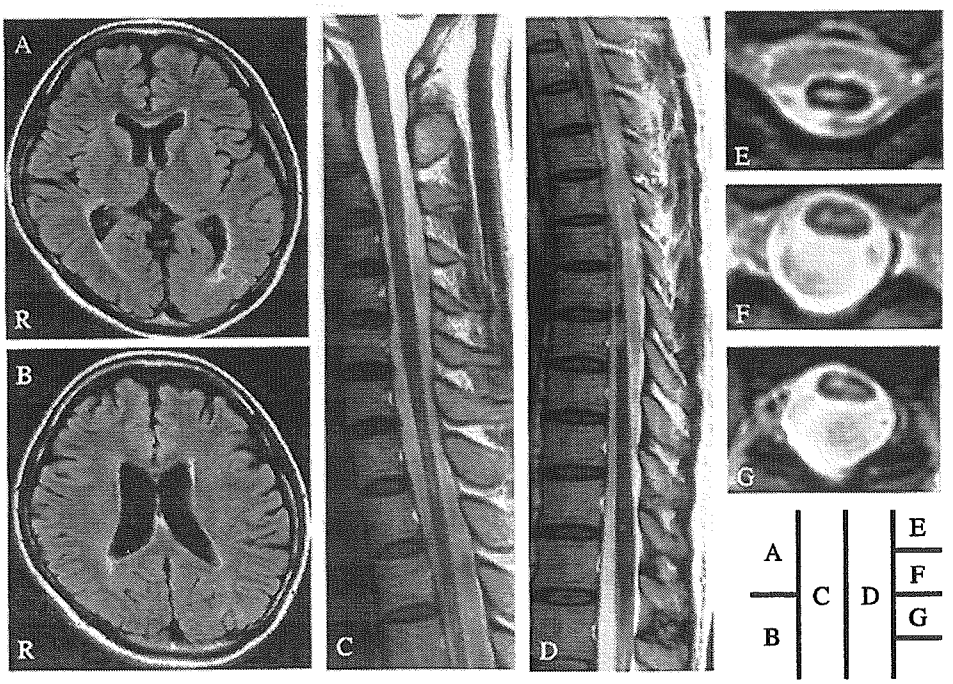

Fig. 1. Representative brain (A, B) and spinal cord MRI (C–G) of a typical OS-MS patient at relapse (disease duration: 4 years). No lesion is visible on T2-weighted axial images of the brain. Longitudinally extensive spinal cord lesion at Th2 to 7 spine levels is shown in T2-weighted sagittal (C, D) and axial (E–G) images of the spinal cord (E: Th1, F: Th3–4 and G: Th4–5 spine levels).

significance. EDSS scores at remission or convalescence did not differ significantly between the two groups.

On brain MRI, the frequency of nine or more T2-hyperintense lesions was significantly higher in C-MS than OS-MS ($p=0.0006$) (Table 1) (Fig.1A and B). Moreover, the frequency of at least three periventricular lesions was also significantly higher in C-MS than OS-MS ($p=0.0015$). However, the frequencies of juxtacortical and infratentorial lesions and gadolinium-enhanced lesions were not significantly different between the two subgroups. Thus, the proportion of patients who fulfilled McDonald's MRI criteria was significantly higher in C-MS than OS-MS ($p=0.0098$). On brain MRI, the frequency of T1 black hole lesions was significantly lower in OS-MS than in C-MS ($p=0.0046$).

On spinal cord MRI, the frequencies of spinal cord lesions were similar between OS-MS and C-MS. The lengths of the spinal cord lesions on MRI were longer in OS-MS than C-MS, though the difference did not reach a statistical significance, and the frequency of longitudinally extensive spinal cord lesions was significantly higher in OS-MS than C-MS ($p=0.0398$) (Table 1) (Fig. 1C–G). Even when seven patients on low dose corticosteroid at the time of blood sampling (4 OS-MS and 3 C-MS) were excluded, essentially the same results were obtained in respect to comparisons between the two subtypes (data not shown).

3.2. Vascular growth factor levels

Serum VEGF concentration was significantly higher in MS patients in relapse (320.5±316.1 pg/ml, mean±S.D.) than in controls (147.3±136.4 pg/ml) ($p=0.0495$) and those in remission (48.6±25.7 pg/ml) ($p=0.0003$) (Fig. 2A). Even when MS patients on the low dose corticosteroids were omitted, the difference between those in relapse and remission was still significant ($p=0.0021$) and the comparison between MS patients in relapse and controls showed a tendency ($p=0.0807$). We then compared serum VEGF levels among OS-MS at relapse, OS-MS at remission, C-MS at relapse, C-MS at remission and healthy controls; a statistically significant difference was found only between C-MS at relapse and at remission, but not in any other comparisons. The difference between OS-MS in relapse and OS-MS in remission lost statistical significance after correction by multiplying the number of comparisons (Fig. 2B). The difference between OS-MS and C-MS patients in relapse also did not reach statistical significance due to the small sample size, although the former was higher (365.0±387.6 vs. 251.2±148.0 pg/ml).

Basic FGF levels did not differ significantly among MS patients in relapse (5.3±4.7 pg/ml), those in remission (5.4±4.2 pg/ml) and controls (3.7±2.5 pg/ml) (Fig. 3A).

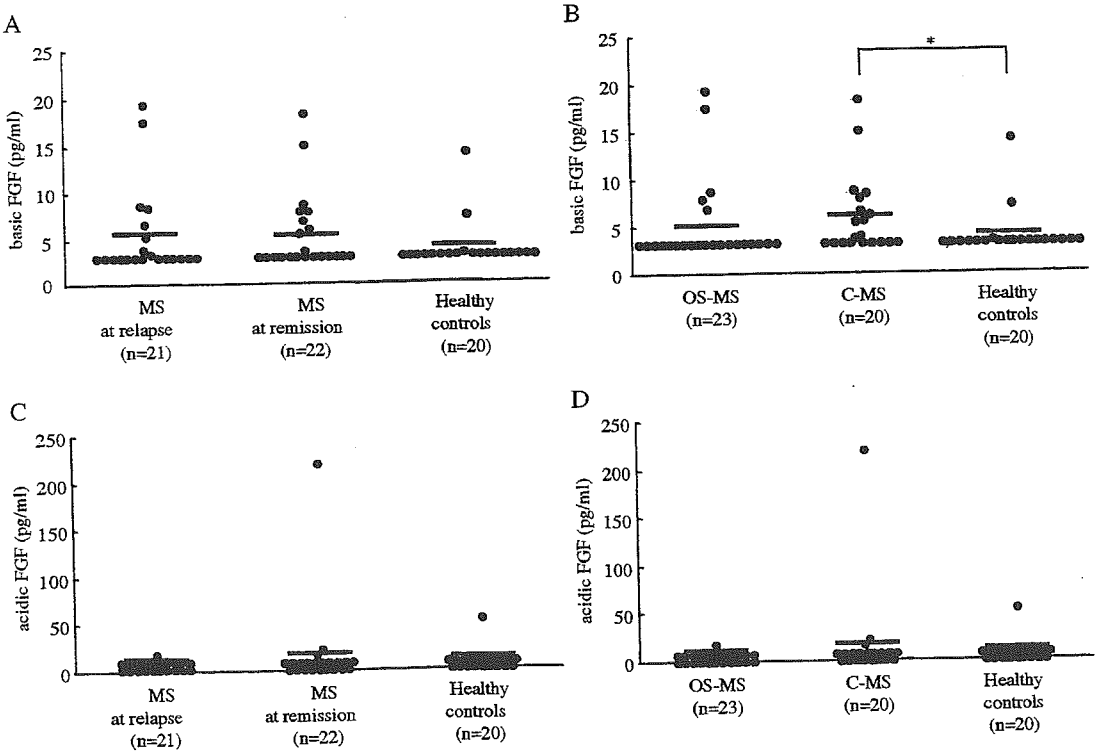

Fig. 3. (A) Basic FGF concentration in sera from MS patients analyzed separately according to their clinical phase. Bars indicate the mean of each group. (B) Basic FGF concentration in sera from MS patients analyzed separately according to their clinical subtype. Bars indicate the mean of each group. *$p<0.05$. (C) Acidic FGF concentration in sera from MS patients analyzed separately according to their clinical phase. Bars indicate the mean of each group. (D) Acidic FGF concentration in sera from MS patients analyzed separately according to their clinical subtypes. Bars indicate the mean of each group.

However, C-MS patients showed a small but significant increase in basic FGF compared with controls (5.8±4.2 vs. 3.7±2.5 pg/ml, $p=0.0291$), irrespective of clinical phase, while no significant change was found in OS-MS patients (5.0±4.5 pg/ml) (Fig. 3B). The difference was still significant even when MS patients on low dose corticosteroids were omitted ($p=0.0189$). No significant changes were detected in any of the other growth factors according to either clinical phase or MS subtype for controls, total MS patients, OS-MS patients, C-MS patients, those in relapse, and those in remission: 8.0±10.4, 24.5±90.7, 6.2±2.3, 45.6±21.2, 6.2±2.5, 41.9±125.7 pg/ml for acidic FGF; 175.2±241.9, 198.4±153.6, 199.8±121.9, 196.7±186.8, 211.9±158.4, 185.5±151.4 pg/ml for PDGF-AA; 375.6±348.6, 386.6±482.3, 420.4± 494.9, 347.6± 477.1, 320.1± 453.8, 450.0±510.4 pg/ml for PDGF-AB; and 215.0±289.9, 196.0±191.9, 162.2±162.5, 234.8±218.7, 157.1± 214.2, 233.1±164.3 pg/ml for PDGF-BB, respectively (Fig. 3C, B and Fig. 4). There was a significant positive correlation between acidic and basic FGF ($p=0.0199$) and between PDGF-AB and -BB ($p<0.0001$), but not -AA, while there were no correlations between VEGF and any other vascular growth factor.

3.3. Correlation among vascular growth factor levels, clinical features and neuroimaging findings

As shown in Fig. 5, when vascular growth factor levels were plotted against the time interval between the onset day of relapse and blood sampling, only VEGF showed a sharp rise at the time of relapse (within one month after the onset). One OS-MS patient whose VEGF levels were

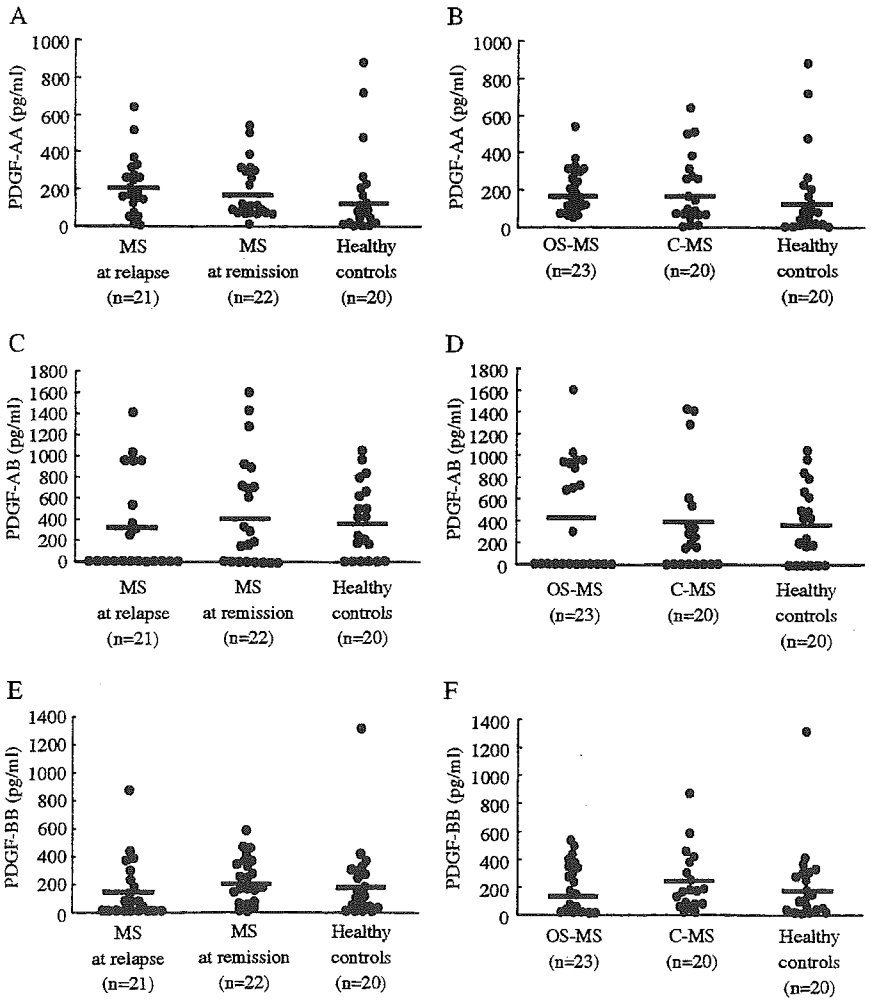

Fig. 4. (A) PDGF-AA concentration in sera of MS patients analyzed separately according to their clinical phase. Bars indicate the mean of each group. (B) PDGF-AA concentration in sera of MS patients analyzed separately according to their clinical subtype. Bars indicate the mean of each group. (C) PDGF-AB concentration in sera of MS patients analyzed separately according to their clinical phase. Bars indicate the mean of each group. (D) PDGF-AB concentration in sera of MS patients analyzed separately according to their clinical subtype. Bars indicate the mean of each group. (E) PDGF-BB concentration in sera of MS patients analyzed separately according to their clinical phase. Bars indicate the mean of each group. (F) PDGF-BB concentration in sera of MS patients analyzed separately according to their clinical subtype. Bars indicate the mean of each group.

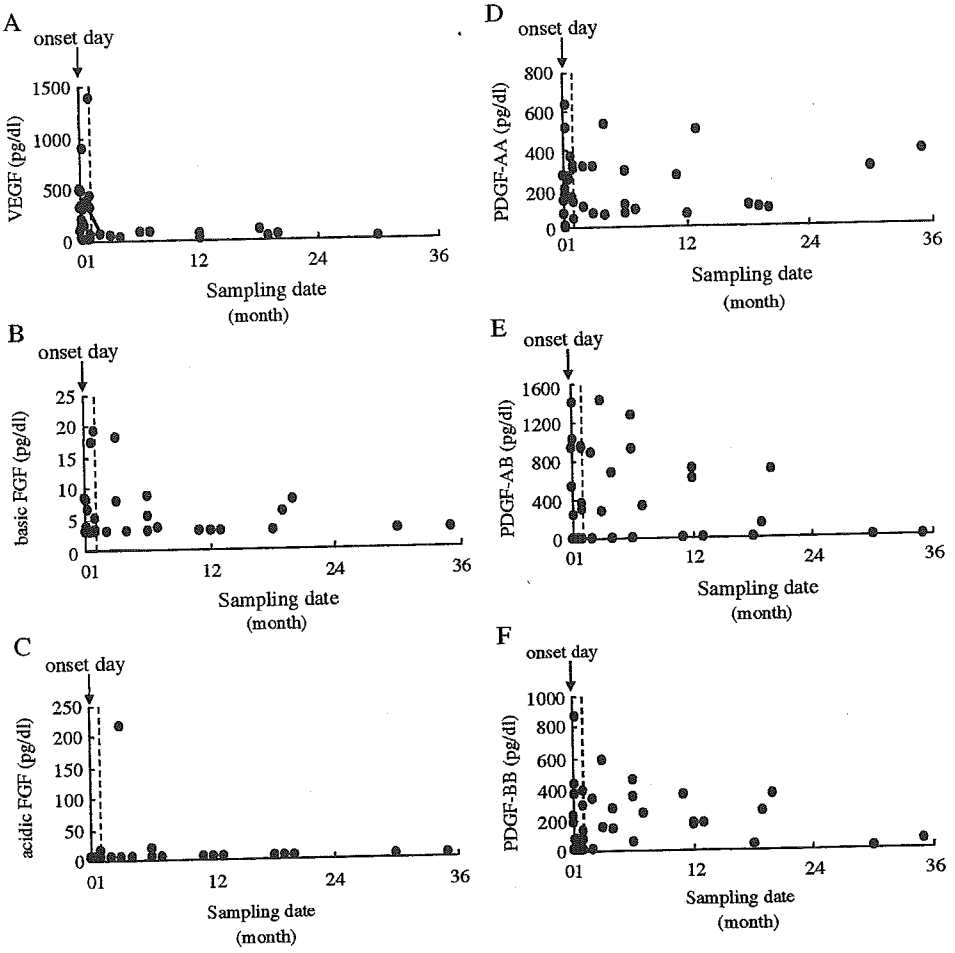

Fig. 5. Vascular growth factor levels against time intervals (months) between the onset day of relapse and blood sampling. (A) VEGF. (B) Basic FGF. (C) Acidic FGF. (D) PDGF-AA. (E) PDGF-AB. (F) PDGF-BB. Relapse phase (broken line) was determined to be within one month after the onset day (arrow). A sharp rise of VEGF levels but not of any others is shown at the time of relapse in MS.

sequentially measured at relapse and remission had elevated VEGF at relapse (333.1 pg/ml) when longitudinally extensive spinal cord lesion was present and showed a decrease in VEGF level in the following remission (67.8 pg/ml) (Figs. 1 and 5). No other vascular growth factors showed such a clear-cut elevation at relapse phase. As the two OS-MS patients with very high VEGF values were also the two oldest patients in the OS-MS group, and both had longitudinally extensive spinal cord lesions, we then analyzed the relationship of vascular growth factor levels with age and MRI findings. A significant positive correlation between VEGF level and age at examination was detected in total MS patients, OS-MS patients, and OS-MS patients in relapse and controls ($r=0.356$ and $p=0.0210$, $r=0.563$ and $p=0.0070$, $r=0.714$ and $p=0.0100$ and $r=0.397$ and $p=0.0296$, respectively), the r value being highest in OS-MS in relapse (Fig. 6). In addition, MS patients at relapse and remission had a similar tendency, yet did not reach statistical significance ($p=0.0579$ and $p=0.0688$, respectively). In OS-MS, there was also a significant positive correlation of VEGF with age at onset ($r=0.459$, $p=0.0279$), but not in C-MS. VEGF had no correlation with disease duration. VEGF at relapse had a significant positive correlation with spinal cord lesion length on MRI in total MS patients ($r=0.506$, $p=0.0319$) (Fig. 7A). However, VEGF in MS patients had no significant correlation with EDSS scores at relapse or convalescence (Fig. 7B). VEGF levels in MS patients with longitudinally extensive spinal cord lesions at relapse were significantly higher than in controls ($p=0.0411$), but not in those without such lesions (Fig. 7C). In contrast, VEGF level had no correlation with the presence of brain MRI lesions (numbers of T2-high and gadolinium-enhanced lesions). Moreover, VEGF level had no correlation with the number of black holes. Even when MS patients on low dose corticosteroids were excluded from statistical analyses, essentially the same results were obtained in respect to VEGF levels and the above-mentioned parameters (data not shown). Neither basic FGF nor any other vascular growth factors examined showed correlation with any

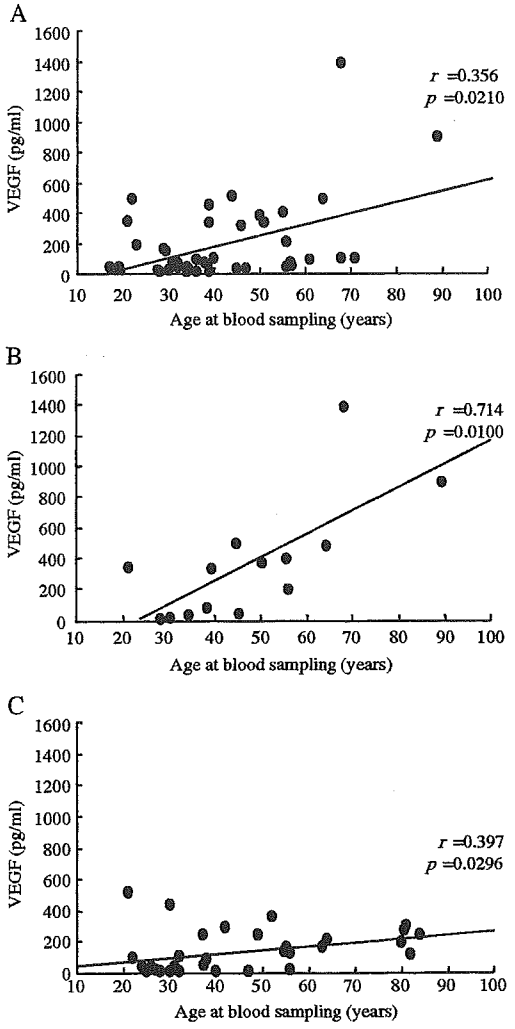

Fig. 6. (A) Relationship between VEGF concentration in sera and age at blood sampling in MS patients. (B) Relationship between VEGF concentration in sera and age at blood sampling in OS-MS patients in relapse. (C) Relationship between VEGF concentration in sera and age at blood sampling in controls.

clinical parameters, including age at onset or examination, disease duration, or MRI findings.

4. Discussion

In the present study, we found that serum VEGF concentrations were significantly elevated in MS patients in relapse compared with controls and those in remission, irrespective of clinical subtype. Furthermore, basic FGF was significantly increased in C-MS patients, irrespective of clinical phase.

In this study, only VEGF was found to be associated with MS relapse. Stockhammer et al. [15] measured serum VEGF in 19 MS patients with unspecified clinical phases and found no elevation. The difference between their results and ours may be explained in part by the sample size and probably the clinical phase of the samples, although exact reasons cannot be clarified as they did not specify the clinical phase of their samples. Proescholdt et al. [7] reported the up-regulation of VEGF in MS lesions as well as in acute lesions with experimental autoimmune encephalomyelitis, an animal model of MS. The results of that study and those in ours strongly suggest that VEGF has a critical role in MS relapse. VEGF is a major mediator of vascular permeability increases as well as angiogenesis [4], and through activation of endothelial cells has been shown to be associated with both acute and chronic inflammation, such as acute allograft rejection [16] and bronchial asthma

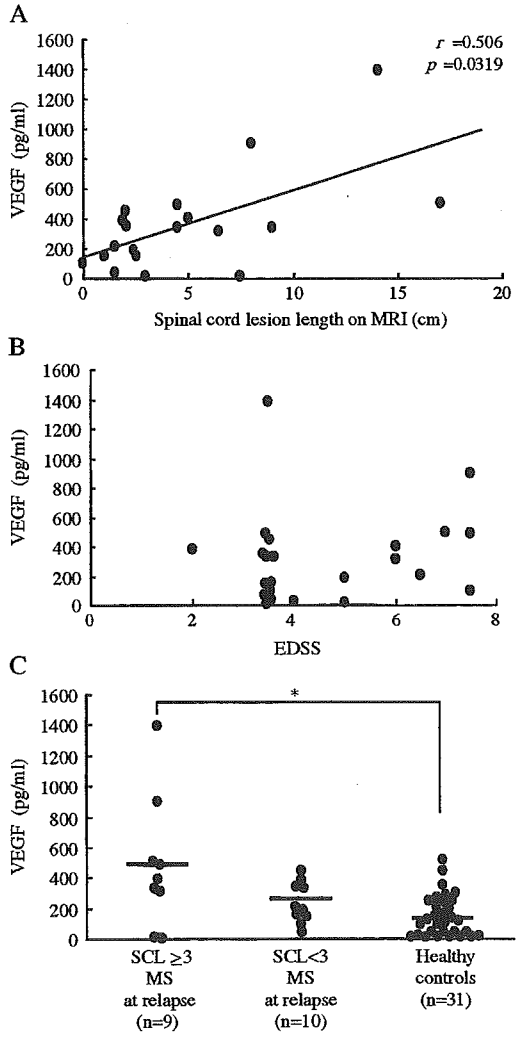

Fig. 7. (A) Relationship between VEGF concentration and spinal cord lesion length (cm) on MRI in MS patients at relapse. (B) Relationship between VEGF concentration and EDSS scores in MS patients at relapse. (C) VEGF concentration in sera from MS patients at relapse analyzed separately according to their spinal cord lesion length on MRI. Bars indicate the mean of each group. SCL≥3: spinal cord lesion length ≥3 vertebral segments, SCL<3: spinal cord lesion length <3 vertebral segments. *$p<0.05$.

[17,18], and vasculopathies, such as diabetic nephropathy [19] and retinopathy [20]. In MS lesions, endothelial cells proliferate [21] and blood vessels show irregular morphology consistent with angiogenesis [3]. Moreover, vascular permeability changes, as shown by serial gadolinium-enhanced MRI studies, precede MS lesion formation [1]. Although not all the sera examined in the present study were obtained at the very beginning of relapse, gadolinium-enhancement of MS lesions usually persists for 3 to 5 weeks [22]; therefore, enhanced VEGF responses at relapse shown here are likely to have contributed to the increased vascular permeability and subsequent endothelial cell proliferation and angiogenesis during relapse. Moreover, VEGF itself is secreted by activated T cells and induces Th1 polarization [23]. As in MS CSF cells where marked upregulation of Th1 cells is seen at relapse [24], VEGF is likely to aggravate inflammation of MS in which Th1 cells are considered to play a crucial role.

Interestingly, VEGF at relapse had a positive correlation with spinal cord lesion length on MRI but not brain MRI findings, and only MS patients with longitudinally extensive spinal cord lesions showed significantly higher VEGF levels compared with controls. These findings suggest that VEGF might contribute to the development of severe spinal cord lesions. Edema following increased vascular permeability induced by VEGF might lead to focal disturbance of microcirculation with subsequent ischemia and tissue necrosis [2]. Such a mechanism might preferentially occur in the spinal cord and optic nerves that have tight and compact structures within narrow bony canals [2].

Therefore, the effects of VEGF might be more deleterious in spinal cord than in brain, which might partly explain the cystic necrosis of tissues frequently seen in Asian MS patients. The lack of correlation between VEGF and EDSS scores might be explained by the fact that the latter are determined by dysfunction in various parts of the CNS. Since genotypes encoding higher VEGF production are reportedly associated with diabetic microvasculopathy [19,20] and acute renal allograft rejection [16], and since significant ethnic differences in polymorphisms of the VEGF gene have also been reported [25], such polymorphisms warrant future investigation in MS patients, especially Asian ones.

In our study, both MS patients in total and controls showed similar weak but significant positive correlations between VEGF and age at blood sampling, while in OS-MS in relapse VEGF and age at examination showed much stronger positive correlations. Although VEGF has been shown to be associated with age-associated diseases, such as neovascular age-related macular degeneration [4,26], no correlation between VEGF and age has previously been reported [27]. However, in these studies, such wide ranging ages as in ours have not been investigated. In general, late-onset MS is associated with faster progression of disability [28], and it has repeatedly been shown that OS-MS has a higher age at onset [10] and thus a higher age at any following relapses, along with greater disability compared with C-MS. In the present MRI study, the spinal cord lesion length also tended to correlate positively with age at examination in MS. Therefore, age-associated increases of VEGF in a general population and thus in MS patients at relapse might in part explain the severe disability and longitudinally extensive spinal cord lesions in OS-MS patients with higher ages at onset and relapse, yet its mechanism remains to be elucidated.

Among other vascular growth factors, only basic FGF was elevated in both acute and stable C-MS patients, which indicates that involvement of other vascular growth factors such as acidic FGF and PDGFs-AA, -AB, and -BB is less likely. A combined increase of VEGF and basic FGF has been reported in inflammatory bowel disease, such as Crohn's disease [28], and liver cirrhosis with spider angiomas [29]. Basic FGF could stimulate the production of VEGF and enhance angiogenesis, and its contribution to neovascularization has been postulated in the above-mentioned conditions [28,29]. However, basic FGF in the present study had no correlation with VEGF level, and no significant change in basic FGF was observed in OS-MS in which angiogenesis is prominent. Basic FGF not only contributes to angiogenesis [6], but it also induces oligodendrocyte progenitor growth in response to demyelination [5]. Therefore, since in C-MS, in which demyelination is prominent and varying degrees of remyelination occur, increases had no relationship with clinical phase and basic FGF levels might reflect host tissue repair rather than vascular changes. Clearly, further large scale studies on these growth factors in cerebrospinal fluid are necessary.

Finally, the proportion of patients who fulfilled McDonald's MRI criteria was significantly lower in OS-MS than C-MS, reflecting the low brain lesion loads that have repeatedly been described in the former [10]. On the other hand, the frequency of longitudinally extensive spinal cord lesions was significantly more common in OS-MS than C-MS. Although the increased VEGF levels at relapse in OS-MS compared with C-MS did not reach statistical significance, extremely high levels of VEGF were only observed in OS-MS patients. Therefore, it is suggested that a certain unique process resulting in distinct distribution of the CNS lesions likely occurs in OS-MS, where VEGF might play various roles.

In summary, we found an elevated VEGF response in MS at relapse, and this had a positive correlation with spinal cord lesion length. Therefore, this might underscore the importance of anti-VEGF therapies, such as those utilizing anti-VEGF monoclonal antibody [30], antisense oligonucleotide [26] and soluble VEGF receptor [31], in MS patients.

Acknowledgements

This work was supported in part by grants from the Ministry of Education, Culture, Sports, Science and

Technology, Japan, the Neuroimmunological Disease Research Committee and the Ministry of Health, Labor and Welfare, Japan, for Research on Brain Science.

References

[1] Kermode AG, Thompson AJ, Tofts P, MacManus DG, Kendall BE, Kingsley DP, et al. Breakdown of the blood–brain barrier precedes symptoms and other MRI signs of new lesions in multiple sclerosis. Pathogenetic and clinical implications. Brain 1990;113:1477–89.
[2] Lassmann H. Hypoxia-like tissue injury as a component of multiple sclerosis lesions. J Neurol Sci 2003;206:187–91.
[3] Kirk S, Frank JA, Karlik S. Angiogenesis in multiple sclerosis: is it good, bad or an epiphenomenon? J Neurol Sci 2004;217:125–30.
[4] Ferrara N. Vascular endothelial growth factor: basic sciences and clinical progress. Endocr Rev 2004;25:581–611.
[5] Frost EE, Nielsen JA, Le TQ, Armstrong RC. PDGF and FGF2 regulate oligodendrocyte progenitor responses to demyelination. J Neurobiol 2003;54:457–72.
[6] Distler JH, Hirth A, Kurowska-Stolarska M, Gay RE, Gay S, Distler O. Angiogenic and angiostatic factors in the molecular control of angiogenesis. Q J Nucl Med 2003;47:149–61.
[7] Proescholdt MA, Jacobson S, Tresser N, Oldfield EH, Merrill MJ. Vascular endothelial growth factor is expressed in multiple sclerosis plaques and can induce inflammatory lesions in experimental allergic encephalomyelitis rats. J Neuropathol Exp Neurol 2002;61:914–25.
[8] Tabira T, Tateishi J. Neuropathological features of MS in Japan. In: Kuroiwa Y, Kuraland LT, editors. Multiple sclerosis east and west. Fukuoka: Kyushu University Press, 1982. p. 273–95.
[9] Ikuta F, Koga M, Takeda S, Ohama E, Takeshita I, Ogawa H, et al. Comparison of MS pathology between 70 American and 75 Japanese autopsy cases. In: Kuroiwa Y, Kuraland LT, editors. Multiple sclerosis east and west. Fukuoka: Kyushu University Press, 1982. p. 297–306.
[10] Kira J. Multiple sclerosis in the Japanese population. Lancet Neurol 2003;2:117–27.
[11] McDonald WI, Compston A, Edan G, Goodkin D, Hartung HP, Lublin FD, et al. Recommended diagnostic criteria for multiple sclerosis: guidelines from the International Panel on the diagnosis of multiple sclerosis. Ann Neurol 2001;50:121–7.
[12] Kira J, Kanai T, Nishimura Y, Yamasaki K, Matsushita S, Kawano Y, et al. Western versus Asian types of multiple sclerosis: immunogenetically and clinically distinct disorders. Ann Neurol 1996;40:569–74.
[13] Kurtzke JF. Rating neurologic impairment in multiple sclerosis: an expanded disability status scale (EDSS). Neurology 1983;33: 1444–52.
[14] Osoegawa M, Miyagishi R, Ochi H, Nakamura I, Niino M, Kikuchi S, et al. Platelet-activating factor receptor gene polymorphism in Japanese patients with multiple sclerosis. J Neuroimmunol 2005;161: 195–8.
[15] Stockhammer G, Poewe W, Burgstaller B, Deisenhammer F, Muigg A, Kiechl S, et al. Vascular endothelial growth factor in CSF. A biological marker for carcinomatous meningitis. Neurology 2000;54:1670–5.
[16] Shahbazi M, Fryer AA, Pravica V, Brogan IJ, Ramsay HM, Hutchinson IV, et al. Vascular endothelial growth factor gene polymorphisms are associated with acute renal allograft rejection. J Am Soc Nephrol 2002;13:260–4.
[17] Hoshino M, Nakamura Y, Hamid QA. Gene expression of vascular endothelial growth factor and its receptors and angiogenesis in bronchial asthma. J Allergy Clin Immunol 2001;107:1034–8.
[18] Kanazawa H, Hirata K, Yoshikawa J. Involvement of vascular endothelial growth factor in exercise induced bronchoconstriction in asthmatic patients. Thorax 2002;57:885–8.
[19] Yang B, Cross DF, Ollerenshaw M, Millward BA, Demaine AG. Polymorphisms of the vascular endothelial growth factor and susceptibility to diabetic microvascular complications in patients with type 1 diabetes mellitus. J Diabetes Complications 2003;17:1–6.
[20] Awata T, Inoue K, Kurihara S, Ohkubo T, Watanabe M, Inukai K, et al. A common polymorphism in the 5′-untranslated region of the VEGF gene is associated with diabetic retinopathy in type 2 diabetes. Diabetes 2002;51:1635–9.
[21] Ludwin SK, Henry JM, McFarland H. Vascular proliferation and angiogenesis in multiple sclerosis: clinical and pathogenetic implications. J Neuropathol Exp Neurol 2001;60:505.
[22] Miller DH, Rudge P, Johnson G, Kendall BE, Macmanus DG, Moseley IF, et al. Serial gadolinium enhanced magnetic resonance imaging in multiple sclerosis. Brain 1988;111:927–39.
[23] Mor F, Quintana FJ, Cohen IR. Angiogenesis–inflammation cross-talk: vascular endothelial growth factor is secreted by activated T cells and induces Th1 polarization. J Immunol 2004;172:4618–23.
[24] Ishizu T, Osoegawa M, Mei F-J, Kikuchi H, Tanaka M, Takakura Y. Intrathecal activation of the IL-7/IL-8 axis in opticospinal multiple sclerosis. Brain 2005;128:988–1002.
[25] Abe A, Sato K, Habuchi T, Wang L, Li Z, Tsuchiya N, et al. Single nucleotide polymorphisms in the 3′ untranslated region of vascular endothelial growth factor gene in Japanese population with or without renal cell carcinoma. Tohoku J Exp Med 2002;198:181–90.
[26] Gragoudas ES, Adamis AP, Cunningham Jr ET, Feinsod M, Guyer DR. VEGF inhibition study in ocular neovascularization clinical trial group. Pegaptanib for neovascular age-related macular degeneration. N Engl J Med 2004;351:2805–16.
[27] Shimada K, Baba T, Neugebauer S, Onozaki A, Yamada D, Midorikawa S, et al. Plasma vascular endothelial growth factor in Japanese Type 2 diabetic patients with and without nephropathy. J Diabetes Complications 2002;16:386–90.
[28] DiSabatino A, Ciccocioppo R, Armellini E, Morera R, Ricevuti L, Cazzola P, et al. Serum bFGF and VEGF correlate respectively with bowel wall thickness and intramural blood flow in Crohn's disease. Inflamm Bowel Dis 2004;10:573–7.
[29] Li CP, Lee FY, Hwang SJ, Lu RH, Lee WP, Chao Y, et al. Spider angiomas in patients with liver cirrhosis: role of vascular endothelial growth factor and basic fibroblast growth factor. World J Gastroenterol 2003;9:2832–5.
[30] Rini BI, Halabi S, Taylor J, Small EJ, Schilsky RL. Cancer and Leukemia Group B. Cancer and Leukemia Group B 90206: a randomized phase III trial of interferon-alpha or interferon-alpha plus anti-vascular endothelial growth factor antibody (bevacizumab) in metastatic renal cell carcinoma. Clin Cancer Res 2004;10:2584–6.
[31] Rota R, Riccioni T, Zaccarini M, Lamartina S, Gallo AD, Fusco A, et al. Marked inhibition of retinal neovascularization in rats following soluble-flt-1 gene transfer. J Gene Med 2004;6:992–1002.

ELSEVIER

Journal of the Neurological Sciences xx (2006) xxx – xxx

Journal of the Neurological Sciences

www.elsevier.com/locate/jns

Long-term favorable response to interferon beta-1b is linked to cytokine deviation toward the Th2 and Tc2 sides in Japanese patients with multiple sclerosis

Feng-Jun Mei [1], Manabu Osoegawa [1], Hirofumi Ochi, Motozumi Minohara, Shi Nan, Hiroyuki Murai, Takaaki Ishizu, Takayuki Taniwaki, Jun-ichi Kira *

Department of Neurology, Neurological Institute, Graduate School of Medical Sciences, Kyushu University, Fukuoka 812-8582, Japan

Received 19 April 2005; received in revised form 24 January 2006; accepted 8 February 2006

Abstract

To address the immune mechanism of the long-term beneficial effects of interferon beta (IFN-β), we measured the intracellular cytokine production patterns of IFN-γ, IL-4 and IL-13 in peripheral blood $CD4^+$ and $CD8^+$ T cells, which previously displayed alterations during the early course of IFN-β treatment, in 15 Japanese patients after long-term IFN-β administration. The patients were treated with IFN-β-1b 8×10^6 units given subcutaneously every other day for a mean period of 34.5±5.5 months (range: 26–43 months). During the follow-up period, 6 patients experienced 33 relapses, while the other 9 were relapse-free. The results revealed the following cytokine alterations: (1) type 2 cytokine, such as IL-4 and IL-13, were significantly increased in producing cell percentages in both $CD4^+$ ($p=0.0356$ and $p=0.0007$, respectively) and $CD8^+$ ($p=0.0231$ and $p=0.0170$, respectively) T cells while IFN-γ, a representative type 1 cytokine, was significantly decreased in the absolute producing cell numbers ($p=0.0125$ in $CD4^+$ T cells and $p=0.0022$ in $CD8^+$ T cells) even after approximately 3 years of IFN-β administration; (2) the intracellular IFN-γ / IL-4 ratio tended to decrease in both $CD4^+$ and $CD8^+$ T cells ($p=0.0535$ and $p=0.0783$, respectively), reflecting a strong downmodulation of type 1 cytokine producing cells; and importantly (3) alterations such as the decreased intracellular IFN-γ / IL-4 ratio in $CD4^+$ T cells and increased percentage of $CD8^+$ $IL\text{-}13^+$ T cells compared with the pretreatment levels were only statistically significant in MS patients without relapse during IFN-β therapy ($p=0.0152$ and $p=0.0078$, respectively). Therefore, we consider that cytokine deviation toward the Th2 and Tc2 sides is linked to a long-term favorable response to IFN-β, while a higher intracellular IFN-γ / IL-4 ratio is associated with treatment failure.

Keywords: Multiple sclerosis; Interferon-β; Interferon-γ; Interleukin-4; Interleukin-13; Th1; Th2

1. Introduction

Multiple sclerosis (MS) is an inflammatory demyelinating disease of the central nervous system (CNS) that is generally considered to be mediated by myelin-autoreactive T cells. Interferon beta (IFN-β) reduces the frequency and severity of clinical relapses in relapsing–remitting MS, and the basis of these beneficial effects has been extensively studied both in vivo and in vitro.

The effects of IFN-β on the cytokine production pattern is especially important, since increasing evidence suggests that MS is largely caused by $CD4^+$ T helper 1 (Th1) cells that produce interferon gamma (IFN-γ) but not interleukin (IL)-4 [1]. Moreover, important roles of $CD8^+$ T cells have also been suggested by the selective enrichment of memory $CD8^+$ T cells in the cerebrospinal fluid (CSF) of MS patients [2] together with diffuse infiltration of clonally expanded $CD8^+$ T cells into the brain parenchyma [3,4]. However, most previous cytokine studies on the effects of IFN-β have been performed within 1 year after initiation of the therapy [5–10], although the beneficial effects of IFN-β persist for

* Corresponding author. Tel.: +81 92 642 5340; fax: +81 92 642 5352.
E-mail address: kira@neuro.med.kyushu-u.ac.jp (J. Kira).
[1] These authors contributed equally to this work.

0022-510X/$ - see front matter © 2006 Elsevier B.V. All rights reserved.
doi:10.1016/j.jns.2006.02.008

several years [11]. Thus, although the long-term beneficial effects of IFN-β are well established, the basis of these effects in vivo remains to be fully elucidated. We recently performed sequential measurements of multiple cytokine production patterns in both $CD4^+$ and $CD8^+$ T cells from the pretreatment period up to 48 months after initiation of the therapy, and found early increases in Th2 cytokines, such as IL-4 and IL-13, followed by late decreases in Th1 cytokines, such as IFN-γ, in both conventional MS (C-MS) and opticospinal MS (OS-MS) [12]. In the present study, we focused on the cytokines that displayed significant alterations in our previous study and evaluated the long-term effects of IFN-β on the cytokine production patterns in $CD4^+$ and $CD8^+$ T cells in the peripheral blood of MS patients several years after initiation of the drug treatment.

2. Materials and methods

2.1. Patients

Fifteen Japanese patients (8 women and 7 men; mean age±SD: 42.13±12.44 years) with relapsing–remitting MS, diagnosed according to the revised diagnostic criteria for MS [13] and treated with IFN-β-1b (Betaferon®; Shering) 8×10^6 units given subcutaneously every other day for at least 2 years (mean period±SD: 34.5±5.5 months; range: 26–43 months), were included in this study. At the time of their enrollment, none of the patients were experiencing an acute attack or had been under immunosuppressive treatment for at least the previous 3 months. The patients were clinically classified into two subtypes: C-MS (13 patients) and OS-MS (2 patients), as described previously [14]. Briefly, patients who had both optic nerve and spinal cord involvement without any clinical evidence of disease in either the cerebrum or the cerebellum were considered to have OS-MS. Patients with minor brainstem signs, such as transient double vision or gaze nystagmus, were included in this subtype. All other patients showing disseminated involvement of the CNS were considered to have C-MS. The demographic features of the patients are shown in Table 1.

2.2. Intracellular cytokine analysis by flow cytometry

The intracellular cytokine patterns were studied by flow cytometry, as described previously [12]. IFN-γ was examined as a Th1 cytokine, while IL-4 and IL-13 were investigated as Th2 cytokines. Peripheral blood mononuclear cells were collected from the patients before treatment and after 2–3 years of IFN-β-1b therapy, and treated with 25 ng/ml phorbol 12-myristate 13-acetate (Sigma, St. Louis, MO), 1 μg/ml of ionomycin (Sigma) and 10 μg/ml brefeldin A (Sigma) for 4 h. The monoclonal antibodies used were: PC5-conjugated anti-CD4 (13B8.2; Becton Dickinson, San Jose, CA), PC5-conjugated anti-CD8 (B9.11; Becton Dickinson), FITC-conjugated anti-IFN-γ (25723.11; Becton Dickinson), PE-conjugated anti-IL-4 (3010.211; Becton Dickinson) and PE-conjugated anti-IL-13 (JES10-5A2; PharMingen, San Diego, CA). The percentages of cytokine-positive $CD4^+$ and $CD8^+$ cells were determined as the % cytokine-positive $CD4^+$ population/total $CD4^+$ population and the % cytokine-positive $CD8^+$ population/total $CD8^+$ population, respectively. Pretreatment measures of cytokine production were done twice at distinct time (average 3.1 days apart) in all MS patients and 9 of 15 in post-treatment measures and means were used when measured twice. According to the results of a preliminary study using 15 subjects, interassay variabilities were as follows; 14.2% in $CD4^+IL\text{-}4^+IFN\text{-}\gamma^-$ cell percentage, 11.6% in $CD4^+IL\text{-}4^-IFN\text{-}\gamma^+$ cell percentage, 29.0% in $CD4^+IL\text{-}13^+$ cell percentage, 13.8% in $CD8^+IL\text{-}4^+IFN\text{-}\gamma^-$ cell percentage, 28.2% in $CD8^+IL\text{-}4^-IFN\text{-}\gamma^+$ cell percentage, 42.1% in $CD8^+IL\text{-}13^+$ cell percentage.

2.3. Statistical analysis

Statistical analyses comparing age at baseline, disease duration at baseline and EDSS scores were performed by the Mann–Whitney *U*-test, while those for the gender ratio were carried out by the Fisher's exact probability test. Statistical analyses comparing the cell percentage and ratio of intracellular cytokine-producing $CD4^+$ and $CD8^+$ T cells between responders and non-responders were performed by the Mann–Whitney *U*-test, and those comparing the cell

Table 1
Demographic features of the 15 MS patients before and during IFN-β-1b treatment

	Total	Non-relapsed	Relapsed
Number of patients	15	9	6
Gender (male : female)	8 : 7	6 : 3	2 : 4
Age at baseline (mean±S.D.)[a]	42.13±12.44	40.33±10.92	44.83±15.09
Disease duration at baseline (mean±S.D.)[a]	5.42±3.64	4.30±2.92	7.11±4.22
EDSS at baseline (mean±S.D.)	4.03±2.18	3.94±2.48	4.17±1.86
EDSS after the observation period (mean±S.D.)	4.27±2.27	4.22±2.59	4.33±1.72
Relapse rate during the 2 years before IFN-β-1b (mean S.D.)	3.00±2.24	2.56±1.88	3.67±2.73
Relapse rate during 1 year of IFN-β-1b (mean±S.D.)	0.73±1.38	0.00±0.00	1.83±1.72
Relapse rate during 1–2 years of IFN-β-1b (mean±S.D.)	1.07±1.67	0.00±0.00	2.67±1.63
Relapse rate during 2–3 years of IFN-β-1b (mean±S.D.)	0.40±0.63	0.00±0.00	1.00±0.63

[a] Years.

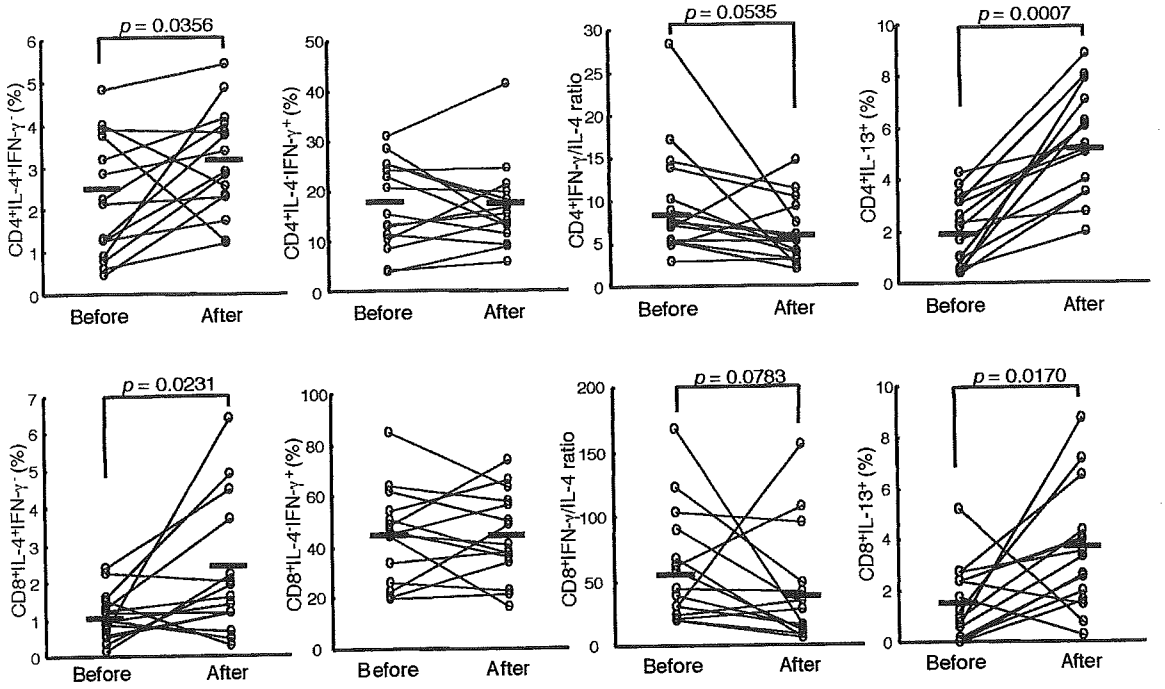

Fig. 1. Changes in the percentages and ratios of intracellular cytokine-producing $CD4^+$ (upper row) and $CD8^+$ (lower row) T cells before treatment and after 2–3 years of IFN-β-1b therapy. Data obtained from the same patient at different times are connected with a line. The bar indicates the mean value at each time point. The total number of MS patients is 15.

percentage and ratio of intracellular cytokine-producing $CD4^+$ and $CD8^+$ T cells between pre-treatment and after-treatment were performed by the Wilcoxon's rank test. A p value of less than 0.05 was considered significant.

3. Results

3.1. Clinical responses to IFN-β therapy

During the 2–3 year observation period, 6 patients suffered 33 relapses: 1 patient experienced 10 relapses, 1 experienced 8 relapses, 1 experienced 5 relapses, 2 experienced 4 relapses and 1 experienced 2 relapses. The remaining 9 patients did not have any relapses during the follow-up period. During this period, 5 of 13 (38%) C-MS patients and 1 of 2 (50%) OS-MS patients relapsed. The gender ratio, age at baseline, EDSS scores and annual relapse rate before initiation of the IFN-β-1b therapy did not differ significantly between the relapsed and non-relapsed patients.

3.2. Intracellular cytokines in $CD4^+$ T cells

In all 15 patients, the percentage of intracellular $CD4^+IL\text{-}4^+IFN\text{-}\gamma^-$ T cells was significantly increased after 2–3 years of IFN-β treatment compared with the pretreatment level

Table 2
Changes in the absolute numbers of intracellular cytokine-producing $CD4^+$ and $CD8^+$ T cells before treatment and after 2–3 years of IFN-β-1b therapy

	$CD4^+$			$CD8^+$		
	$IL\text{-}4^+IFN\text{-}\gamma^-$	$IL\text{-}4^-IFN\text{-}\gamma^+$	$IL\text{-}13^+$	$IL\text{-}4^+IFN\text{-}\gamma^-$	$IL\text{-}4^-IFN\text{-}\gamma^+$	$IL\text{-}13^+$
Before treatment	12.1±10.0	91.9±73.6	38.3±25.2	4.4±2.6	192.3±147.6	30.5±31.4
After treatment	9.5±7.5	50.2±56.2*	62.1±35.8*	4.4±4.8	88.1±65.4**	45.0±43.3 (/μl)
Non-relapsed						
Before treatment	14.4±10.8	92.5±59.7	41.5±25.2	5.0±3.0	163.5±87.3	32.7±32.8
After treatment	10.7±7.4	36.0±20.6*	70.9±32.9*	4.4±3.8	72.7±42.0**	55.0±48.3 (/μl)
Relapsed						
Before treatment	8.6±8.5	91.0±97.2	33.6±26.7	3.5±1.9	235.4±212.2	27.1±31.8
After treatment	7.7±8.0	71.6±85.1	49.0±38.8	4.4±6.5	111.1±90.1	29.9±32.5 (/μl)

* :$p<0.05$ (vs. before IFN-β-1b therapy).

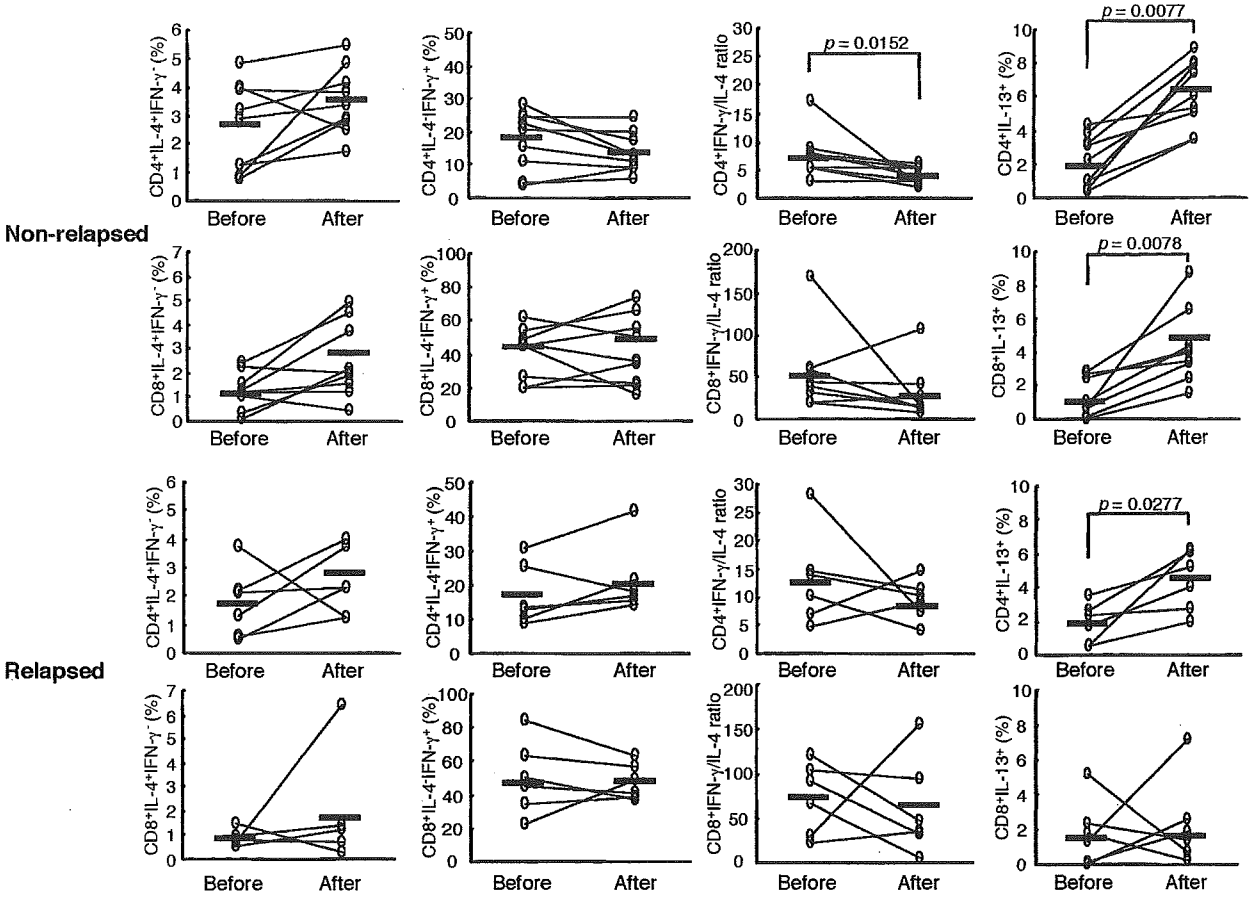

Fig. 2. Changes in the percentages and ratios of intracellular cytokine-producing $CD4^+$ and $CD8^+$ T cells according to the presence or absence of relapses during IFN-β-1b therapy. Data obtained from the same patient at different times are connected with a line. The bar indicates the mean value at each time point. There are 9 non-relapsed patients (upper panel) and 6 relapsed patients (lower panel).

($p=0.0356$) (Fig. 1). A similar significant augmentation pattern was observed for the percentage of intracellular $CD4^+IL\text{-}13^+$ T cells ($p=0.0007$). These changes were beyond the ranges of interassay variability (+ 62.8% in $CD4^+IL\text{-}4^+IFN\text{-}\gamma^-$ T cell percentages and + 165.3% in $CD4^+IL\text{-}13^+$ T cell percentage). The percentage of intracellular $CD4^+IL\text{-}4^-IFN\text{-}\gamma^+$ T cells did not change significantly with IFN-β treatment. Thus, the intracellular IFN-γ / IL-4 ratio tended to decrease after 2–3 years of treatment, but the decrease did not achieve statistical significance ($p=0.0535$) due to the small sample size. With respect to absolute cell numbers, decrease in $CD4^+IL4^-IFN\gamma^+$ T cells after treatment was statistically significant ($p=0.0125$) while $CD4^+IL4^+IFN\gamma^-$ T cells did not show a statistically significant changes (Table 2). In addition, $CD4^+IL\text{-}13^+$ T cells also increased significantly in an absolute number after treatment ($p=0.0231$).

3.3. Intracellular cytokines in $CD8^+$ T cells

In all 15 patients, the percentages of intracellular $CD8^+IL\text{-}4^+IFN\text{-}\gamma^-$ and $CD8^+IL\text{-}13^+$ T cells were significantly increased after 2–3 years of treatment compared with the pretreatment values ($p=0.0231$ and $p=0.0170$, respectively) (Fig. 1). These changes also exceeded the ranges of interassay variability (+130.4% in $CD8^+IL\text{-}4^+IFN\text{-}\gamma^-$ T cell percentages and +182.8% in $CD8^+IL\text{-}13^+$T cell percentage). The intracellular IFN-γ / IL-4 ratio tended to decrease after 2–3 years of treatment, but the decrease did not reach statistical significance ($p=0.0783$). Concerning absolute cell numbers, decrease in $CD8^+IL\text{-}4^-IFN\text{-}\gamma^+$ T cells after treatment was statistically significant ($p=0.0022$) while $CD8^+IL\text{-}4^+IFN\text{-}\gamma^-$ T cells did not show a significant change. Increase of $CD8^+IL\text{-}13^+$ T cells after treatment was not statistically significant in an absolute number.

3.4. Clinical responses and cytokine production patterns

The intracellular cytokine expression patterns were compared according to the clinical responses. MS patients without any relapses demonstrated significant decreases in the intracellular IFN-γ / IL-4 ratio in $CD4^+$T cells ($p=0.0152$) and increases in $IL\text{-}13^+$ cell percentages in both $CD4^+$ and $CD8^+$ T cells ($p=0.0077$ and $p=0.0078$,

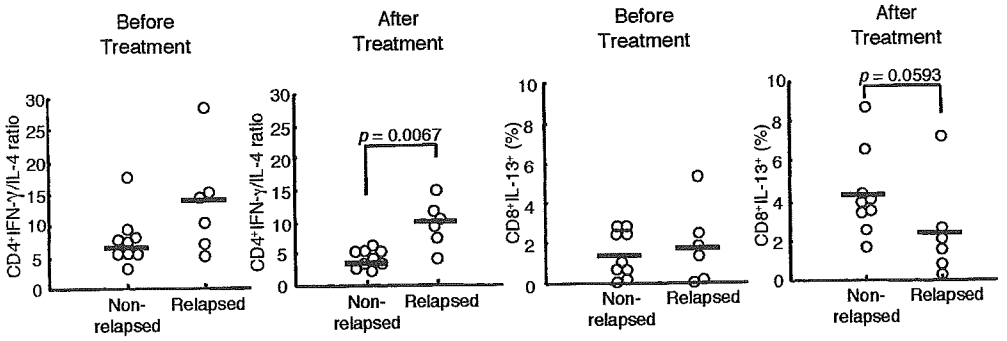

Fig. 3. Comparisons of the ratios of intracellular cytokine-producing $CD4^+$ T cells between relapsed and non-relapsed MS patients before treatment and after 2–3 years of IFN-β-1b therapy. The bar indicates the mean value in each group. There are 9 non-relapsed patients and 6 relapsed patients.

respectively) compared with the pretreatment levels, and patients who underwent relapses showed a significant increase in $CD4^+IL\text{-}13^+$ T cell percentage ($p=0.0277$) (Fig. 2). As to absolute cell numbers, both $CD4^+IL\text{-}4^-IFN\text{-}\gamma^+$ T cells and $CD8^+IL\text{-}4^-IFN\text{-}\gamma^+$ T cells decreased significantly after treatment only in non-relapsed patients ($p=0.0284$ and $p=0.0077$, respectively), but not in relapsed ones (Table 2). Absolute number increase in $CD4^+IL\text{-}13^+$ T cells was significant only in non-relapsed patients ($p=0.0209$) but not in relapsed patients while absolute number of $CD8^+IL\text{-}13^+$ T cells showed a tendency to increase after treatment in non-relapsed patients ($p=0.0858$) but not in relapsed ones.

When the intracellular cytokine expression patterns were compared between MS patients with and without relapses during IFN-β-1b therapy, the pretreatment values did not differ significantly between the two groups for any of the parameters (Fig. 3). However, after 2–3 years of treatment, the relapsed patients tended to have a lower percentage of $CD4^+IL\text{-}4^+IFN\text{-}\gamma^-$ T cells and a higher percentage of $CD4^+IL\text{-}4^-IFN\text{-}\gamma^+$ T cells than the non-relapsed patients ($p=0.0990$ and $p=0.0771$, respectively), resulting in a significantly higher intracellular IFN-γ / IL-4 ratio in $CD4^+$ T cells in the relapsed patients than in the non-relapsed patients ($p=0.0067$). On the other hand, after IFN-β treatment, the non-relapsed patients tended to have a higher percentage of $CD8^+IL\text{-}13^+$ T cells than the relapsed patients ($p=0.0593$). Concerning absolute cell numbers, there was no significant difference in any positive cells examined in either before or after treatment between the two groups (data not shown).

4. Discussion

This study revealed the following long-term effects of IFN-β on the intracellular cytokine production patterns of peripheral blood $CD4^+$ and $CD8^+$ T cells in MS patients: (1) type 2 cytokines, such as IL-4 and IL-13, were significantly increased in producing cell percentages in both $CD4^+$ and $CD8^+$ T cells while IFN-γ, a representative type 1 cytokine, was significantly decreased in the absolute producing cell numbers in both $CD4^+$ and $CD8^+$ T cells, even after approximately 3 years of IFN-β administration; (2) the intracellular IFN-γ / IL-4 ratio tended to decrease in both $CD4^+$ and $CD8^+$ T cells, reflecting a strong downmodulation of type 1 cytokines; and importantly (3) alterations such as the decreased intracellular IFN-γ / IL-4 ratio in $CD4^+$ T cells, increased percentage of $CD8^+IL\text{-}13^+$ T cells and increased cell numbers of $CD4^+IL\text{-}13^+$ T cells were only statistically significant in MS patients who responded well to IFN-β treatment, while the intracellular IFN-γ / IL-4 ratio in $CD4^+$ T cells was significantly higher in the relapsed patients than in the non-relapsed patients after long-term administration of IFN-β. Although each clinical parameter did not differ significantly between non-relapsed (responder) and relapsed (non-responder) patients, a longer disease duration, nevertheless higher relapse rate in the preceding two years before IFN-β initiation and resulting higher EDSS at baseline suggest high disease activity of the non-responders at baseline and could be a factor in the lack of response to IFN-β. Thus, difference in cytokine profile between responders and non-responders may reflect difference in baseline disease activity between the two groups.

Although the present study is an ex vivo study of peripheral blood lymphocytes after stimulation by PMA and ionomycin, the proportions of certain cytokine-producing cells obtained using this assay have been reported to reflect those destined to produce relevant cytokines in vivo [15]. Therefore, the results of the current study are considered to reflect the long-term in vivo effects of IFN-β on the Th1 / Th2 and Tc1 / Tc2 balance in MS.

Various mechanisms have been proposed to explain the beneficial effects of IFN-β treatment for MS. Among these, cytokine alterations probably play key roles, since cytokines are crucial for the induction and maintenance of autoimmune inflammation. Previous studies on the cytokine balance in MS under IFN-β treatment have reported the following conflicting findings: IFN-β-1a decreases IL-12 and augments IL-10 production [7]; IFN-β-1b decreases IFN-γ while IFN-β-1a enhances IL-4 and IL-10 [10]; IFN-β-1a [8] and IFN-β-1b [6] down-modulate both IFN-γ and IL-4 [6]; IFN-β-1b induces no changes in either Th1 or Th2 marker genes [9]; IFN-β-1b increases IFN-γ [5]. These

inconsistent results for the cytokine changes induced by IFN-β in MS probably reflect differences in the methodologies employed and distinct time points examined as well as the complex biology of the cytokines themselves.

To the best of our knowledge, there are no reports in the literature regarding the cytokine changes induced by administration of IFN-β for as long as 3 years. Moreover, cytokine profiles that can discriminate between favorable and unfavorable responses to long-term administration of IFN-β have not been clarified in detail. Although the number of MS patients who were successfully followed-up in the present study was not large, we found a significant decrease in the production of type 1 cytokine, IFN-γ, and relative increase in the production of type 2 cytokines, such as IL-4 and IL-13, in both $CD4^+$ and $CD8^+$ T cells, even after long-term treatment with IFN-β, suggesting that shift towards of Th2 and Tc2 sides is one of the major in vivo effects of IFN-β. On the other hand, an increase in type 1 cytokines, such as IFN-γ, was observed in a fraction of MS patients in the first few weeks in our previous study [12] and in the first 2 months by Dayal et al. [5], and this was not related to an increased number of relapses. However, in the late stage of IFN-β therapy, the present study revealed a significant difference in the intracellular IFN-γ / IL-4 ratio between relapsed and non-relapsed patients, with a higher ratio being associated with relapses. Therefore, a down-modulation of Th1 response with relative increase of Th2 response, which lowers the intracellular IFN-γ / IL-4 ratio, is considered to be critical for maintaining a relapse-free state under long-term IFN-β therapy.

Concerning $IL\text{-}13^+$ cells, their increase among $CD4^+$ T cells and $CD8^+$ T cells after long-term IFN-β administration was more pronounced in the non-relapsed patients than in the relapsed patients. These observations may indicate that a favorable response to IFN-β is linked to an elevation of $CD4^+IL\text{-}13^+$ T cells and $CD8^+IL\text{-}13^+$ T cells. We previously reported unexpected increases in $CD4^+IL\text{-}13^+$ and $CD8^+IL\text{-}13^+$ T cells at relapse in MS, especially in C-MS [16], the roles for which required clarification by further studies. The results of the present study suggest that these $IL\text{-}13^+$ cells may have a protective role, since the increase in $IL\text{-}13^+$ cells was associated with a decrease in the relapse rate. Therefore, the increase in these cells observed at relapse may be the host's efforts to overcome Th1-mediated inflammatory processes. The recent observation that $CD8^+$ T cells producing IL-13 were correlated negatively with T1 lesion loads on brain magnetic resonance imaging in MS [17] further suggests a role of $CD8^+$ suppressor cells in down-regulating the disease activity, and supports a protective role for $CD8^+IL\text{-}13^+$ T cells. IL-13 shares some receptor components with IL-4 and demonstrates similar functions to IL-4 [18]. IL-4 and IL-13 mostly act synergistically in the down-regulation of Th1 cells, although increasing evidence indicates that IL-13 rather than IL-4 plays a crucial role in many aspects of immune regulation. For example, IL-13 is essential for tolerance induction [19], renders T cells unresponsive to IL-12 [20] and decreases TNF-α-mediated cytotoxicity [21]. Although the mechanism of the protective action of IL-13 in MS remains to be clarified, an increase in the number of $IL\text{-}13^+$ cells could be one of the biomarkers for IFN-β responsiveness in MS.

In our previous study, similar cytokine changes during IFN-β therapy were noted in both OS-MS and C-MS [12] and it was suggested that the IFN-β action may have a common mechanism in the two MS subtypes, at least in the early course of the treatment. In the present study, the number of OS-MS patients was limited and further studies in a larger scale are necessary to address subtype-specific changes in the late phase of IFN-β therapy.

In summary, the results of the current study have revealed that alterations in the cytokine balance, such as a decreased intracellular IFN-γ / IL-4 ratio in $CD4^+$ T cells and an increase in $CD4^+IL\text{-}13^+$ T cells and $CD8^+IL\text{-}13^+$ T cells, are linked with a favorable response to IFN-β, while a higher intracellular IFN-γ / IL-4 ratio is associated with treatment failure after long-term IFN-β therapy in MS.

Acknowledgements

We thank K. Matsuzaki and T. Tanaka for their helpful assistance. This study was supported in part by a Neuroimmunological Disease Research Committee grant and a Research on Brain Science grant from the Ministry of Health, Labor and Welfare of Japan, and Grants-in-Aid from the Ministry of Education, Culture, Sports, Science and Technology of Japan.

References

[1] Martin R, McFarland HF, McFarlin DE. Immunological aspects of demyelinating diseases. Annu Rev Immunol 1992;10:153–87.
[2] Jacobsen M, Cepok S, Quak E, Happel M, Gaber R, Ziegler A, et al. Oligoclonal expansion of memory CD8+ T cells in cerebrospinal fluid from multiple sclerosis patients. Brain 2002;125:538–50.
[3] Gay FW, Drye TJ, Dick GW, Esiri MM. The application of multifactorial cluster analysis in the staging of plaques in early multiple sclerosis. Identification and characterization of the primary demyelinating lesion. Brain 1997;120:1461–83.
[4] Babbe H, Roers A, Waisman A, Lassmann H, Goebels N, Hohlfeld R, et al. Clonal expansions of CD8(+) T cells dominate the T cell infiltrate in active multiple sclerosis lesions as shown by micromanipulation and single cell polymerase chain reaction. J Exp Med 2000;192:393–404.
[5] Dayal AS, Jensen MA, Lledo A, Arnason BGW. Interferon-gamma-secreting cells in multiple sclerosis patients treated with interferon beta-1b. Neurology 1995;45:2173–7.
[6] Furlan R, Bergami A, Lang R, Brambilla E, Franciotta D, Martinelli V, et al. Interferon-beta treatment in multiple sclerosis patients decreases the number of circulating T cells producing interferon-γ and interleukin-4. J Neuroimmunol 2000;111:86–92.
[7] Byrnes AA, McArthur JC, Karp CL. Interferon-β therapy for multiple sclerosis induces reciprocal changes in interleukin-12 and interleukin-10 production. Ann Neurol 2002;51:165–74.
[8] Franciotta D, Zardini E, Bergamaschi R, Andreoni L, Cosi V. Interferon γ and interleukin 4 producing T cells in peripheral blood